



## Improvement of Heat Transfer by Using Porous Media, Nanofluid, and Fins: A Review

Abbas Fadhil Khalaf<sup>1</sup>, Ali Basem<sup>2\*</sup>, Hasan Qahtan Hussein<sup>1</sup>, Ali Kadhim Jasim<sup>1</sup>, Karrar A. Hammoodi<sup>2</sup>, Ammar M. Al-Tajer<sup>2</sup>, Ihab Omer<sup>2</sup>, Mujtaba A. Flayyih<sup>3</sup>

<sup>1</sup> Faculty of Engineering, Kerbala University, Karbala 56001, Iraq

<sup>2</sup> Air Conditioning Engineering Department, Faculty of Engineering, Warith Al-Anbiyaa University, Karbala - Baghdad Rd 56001, Iraq

<sup>3</sup> Biomedical Engineering Department, Al-Mustaqbal University College, Hillah, Babylon, Iraq

Corresponding Author Email: [ali.basem@g.uowa.edu.iq](mailto:ali.basem@g.uowa.edu.iq)

<https://doi.org/10.18280/ijht.400218>

### ABSTRACT

**Received:** 29 March 2022

**Accepted:** 20 April 2022

#### **Keywords:**

*nanofluid, porous media, fins, heat transfer*

The world's interest in energy and as a result of the urgent importance of that, researchers focused on the development of heat transfer to have a significant impact on the consumption of that energy. Where we note the great interest by researchers in developing heat transfer and using the best possible methods to improve heat transfer. In this literary review, a large group of research has been carried out to find out the importance of heat transfer and the methods used by researchers to develop heat transfer. Porous materials, nanomaterials and fins were used in the development of heat transfer. Where we note the importance of adding these materials (porous materials, nanomaterials and fins) to the original materials contribute significantly and clearly to improving heat transfer and this has a significant impact on energy consumption or trying to dissipate it, as we note the clear difference when using the original materials without adding these materials as the heat transfer is less and it consumes more time. Researchers can focus on the importance of improving heat transfer for its importance in many applications that have a direct impact on human life.

## 1. INTRODUCTION

The world has recently witnessed a great interest in the use of modern electronic means and anything related to the development that occurred in the recent period. We note the interest in heat transfer as an important element in many scientific applications and has a very large impact on various aspects of life, for example (electronics, optical devices, X-rays, refrigeration devices, etc.). The large and rapid growth of these electronic devices and technologies through miniaturizing these devices, storing data and improving their operating rate led to serious problems in the thermal management of these devices [1]. Where the poor thermal conductivity is one of the most important factors that need to increase the thermal conductivity, and this requires focus and work on using materials that have high thermal conductivity or improving these materials. Because of the importance of the topic in many applications, researchers have paid much attention and tried a lot to find the best and best ways to improve the characteristics of thermal energy transfer [2-5]. Knowing and understanding the heat transfer mechanism is critical to designing many, many wide applications in all areas of industrial, commercial and domestic appliances, including solar energy, air conditioning, the oil and gas industry, power production, and electronic refrigeration [6-8]. The importance of large heat transfers and its wide impact on many applications in human life. Researchers have tried to improve heat transfer in several ways, the most important of which is placing the fins to increase heat transfer or increasing the surface area of materials to increase the area to which heat is

transmitted [9]. It also includes improving heat transfer by improving the heat transfer of porous materials by improving them so that heat is lost and gained at a high speed [10-14]. One of the most important modern methods used to improve heat transfer is adding nanomaterials to heat transfer compounds and significantly improving the ability to lose and gain it at high speed. Where nanomaterials have caused an industrial revolution in several areas, the most important of which is heat transfer due to the importance of this field and its impact in various fields [15-20].

The research aims to present all previous research related to the work of previous researchers in order to improve heat transfer specially by used Porous Media, Nanofluid, and fins, which is an important factor in improving the efficiency of all engineering applications, in order to help other researchers, identify the latest findings of other studies.

## 2. IMPROVE HEAT TRANSFER

Heat transfer is of great importance, as it has many important applications. For this reason, researchers focused on developing heat transfer and finding solutions to increase heat transfer. One of the solutions is to add porous media, nanomaterials and fins, where we will explain the researchers' interest in this review and the results they obtained.

## 3. IMPROVE HEAT TRANSFER BY POROUS MEDIA

Porous materials are utilized as a cheap way to enlarge the

heat transfer area and improve effective thermal conductivity for the purposes of enhancing heat transfer and maximizing energy consumption. Because of their huge surface area per unit volume, porous materials (such as metal foam) play a growing role in heat exchangers. A great deal of effort has gone into improving heat transfer, and a large range of technologies have been created to accomplish so [21]. Heat transport inside phase-changing materials is aided by porous media. The use of metallic foam in a casing and tube to promote heat transfer. The relevance of employing porous materials in increasing heat transmission is demonstrated in Figures 1, 2, 3, where the melting average increases as the porosity of the metal foam decreases due to the extremely effective thermal conductivity. Because of the metal foam's low porosity, the melting process is quick. As the porosity volume decreases, the heat transmission area between the liquid PCM and the metal foam increases, speeding up the melting process [22].

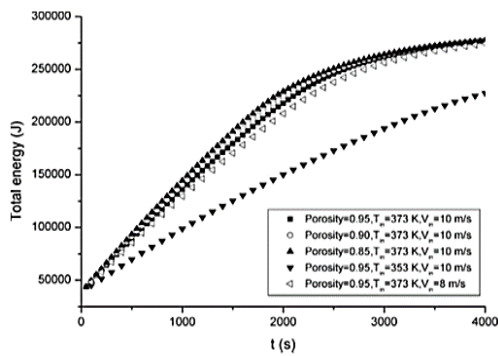


**Figure 1.** Total energy of PCM domain (sensible and latent heat) in the LHTES unit vs. time [22]

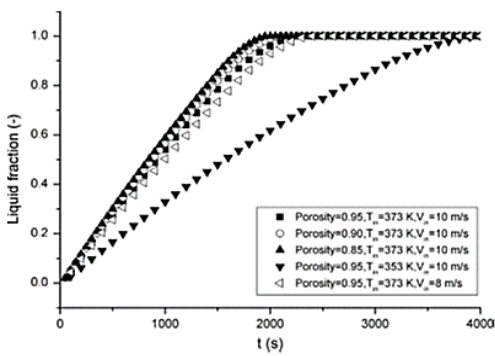


**Figure 2.** Liquid fraction of PCM domain vs. time [22]

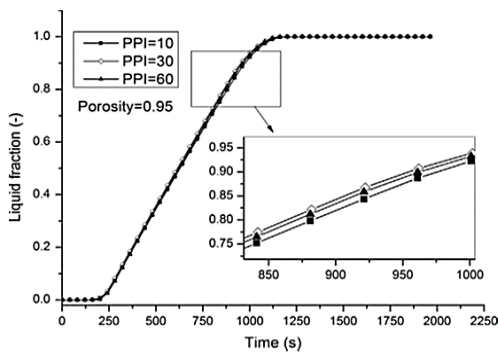


**Figure 3.** Comparison of different pore sizes ( $T_{in}=473$  K and  $V_{in}=10$  m/s) [22]

Porous materials were introduced to improve heat transfer during compression (for a pressure ratio of 10) and expansion (for a pressure ratio of 6) for a pressure ratio of 10. Three intermittent ABS gaskets with 2.5, 5- and 10-mm plate spacing and inserts of aluminum foam with a size of 10 and 40 pores per inch were examined in a compression experiment, as were five examples with varied porous inserts. Stretching experiments were also conducted with 2.5 mm and 5 mm discontinuous plate inserts. The results of this investigation (Figures 4, 5, 6, 7) demonstrate the importance of porous materials in increasing heat transport [23].

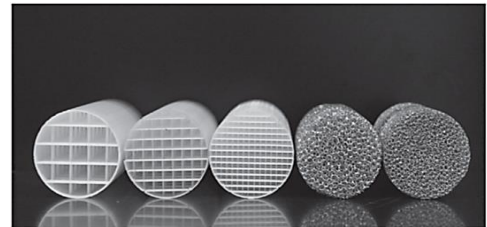


**Figure 4.** Five types of porous inserts used in compression/expansion experiments [23]

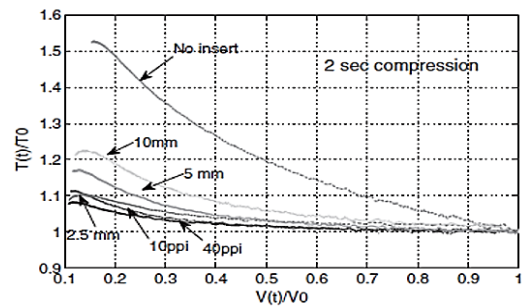


**Figure 5.** Temperature-volume profiles for compression cases with different inserts at similar compression times of 2 s [23]

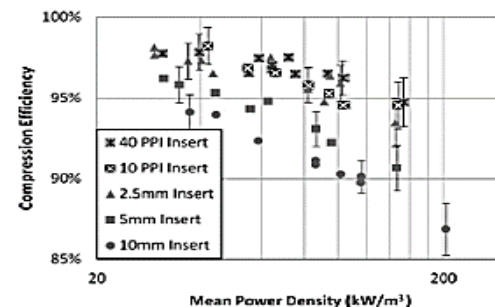
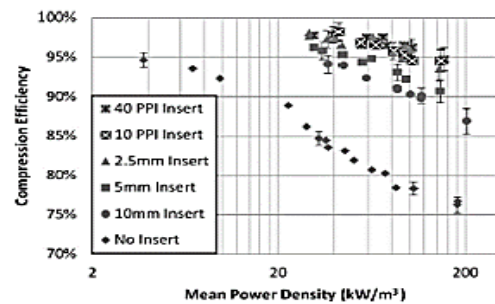


**Figure 6.** Compression coefficient vs compression power density for various inserts (pressure ratio=10). Expanded view of the insert cases [23]

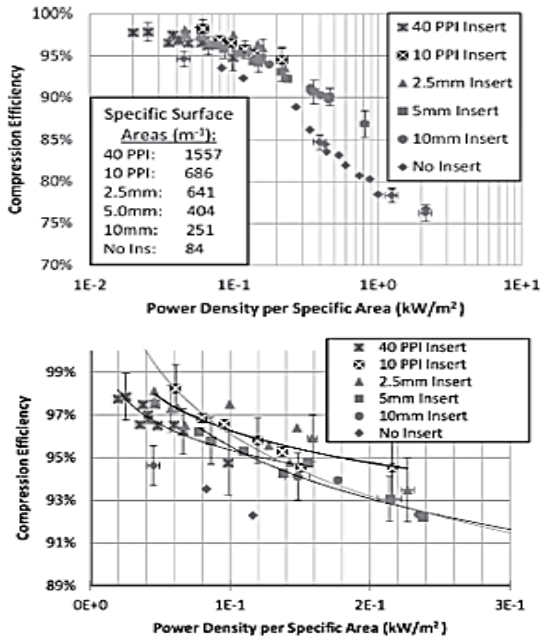


**Figure 7.** Compression coefficient vs compression power density normalized by specific surface area for various inserts and compression times (pressure ratio =10). Expanded view of high efficiency region [23]

We discover that porous materials have a significant effect on improving heat transfer when steady state laminar Ferro convection through a circular horizontal tube partially filled with porous media is examined under continuous heat flux. As both porous media and a magnetic field are used in the flow of magnetized fluids, heat transfer improves by up to 2.4 times when compared to heating the underlying fluid transmission. The findings of this study (Figures 8, 9) demonstrate the importance of porous materials in increasing heat transfer [24].

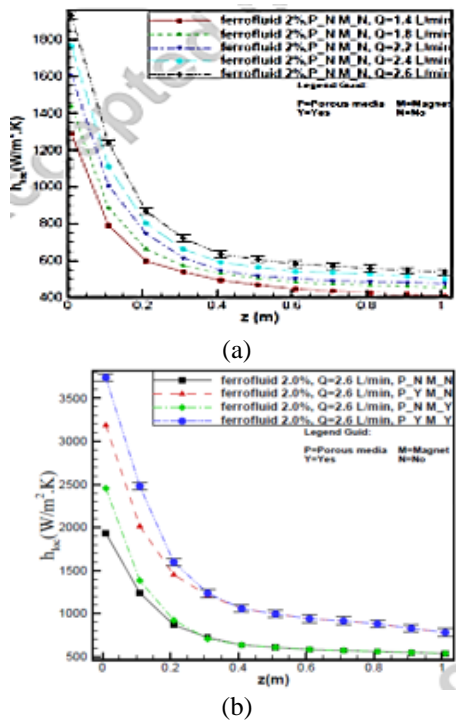


**Figure 8.** Local heat transfer coefficient (a) different flowrate and constant condition (b) constant flowrate and four main different condition [24]

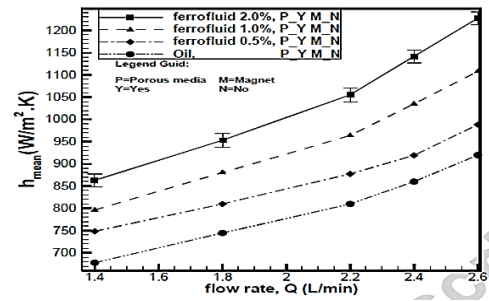


**Figure 9.** Mean (overall) heat transfer coefficient versus flow rate for different volume fractions [24]

The presence of porous media in the flow channel improves the matrix of thermal conductivity and effective flow thermal capacity, as well as the matrix of porous solids, which improves radiation heat transfer, particularly in two-phase flow (gas-water) systems. The presence of porous media in the flow channel improves the thermal conductivity matrix and effective heat capacity of the flow, according to research. The heat transfer velocity is also increased in a porous solid-state environment, especially in systems where gas is moving [25].

Six various thicknesses of the porous media are evaluated to achieve the optimum thickness for the purpose of determining the right thickness of the porous media. Finally, a number of simulation runs are carried out to determine the heat exchanger's minimum needed length for various inlet conditions. The product temperature is reduced by approximately 40% when the porous media is used in the heat exchanger, compared to the standard heat exchanger. As a result, utilizing porous medium in the heat exchanger has a considerable impact on the cooling rate, resulting in greater product quality. When compared to a standard heat exchanger, the length of the porous heat exchanger is reduced by over 35%. The importance can be seen in the Figures 10, 11, 12, and 13 [26].

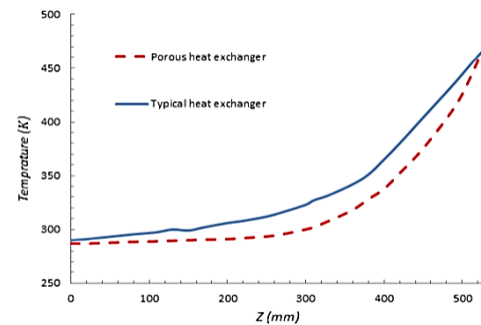


**Figure 10.** Comparison of the porous media in the heat exchanger and typical heat exchanger [26]

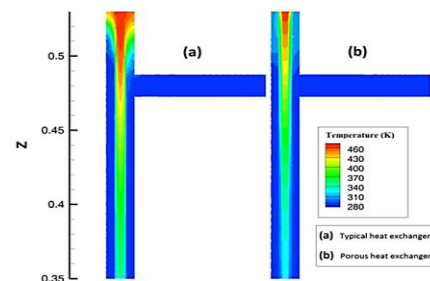


**Figure 11.** Comparison of the porous media in the heat exchanger and typical heat exchanger [26]

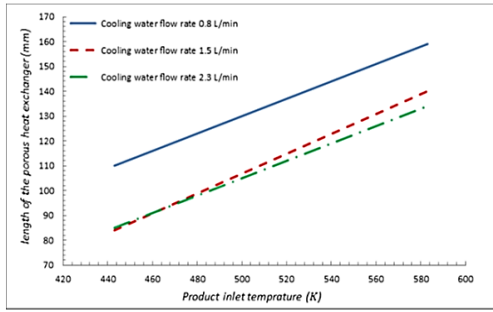


**Figure 12.** Length of the heat exchanger for different product inlet temperatures [26]

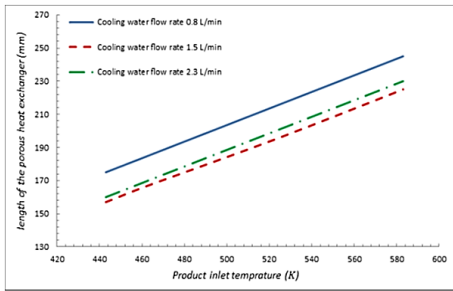
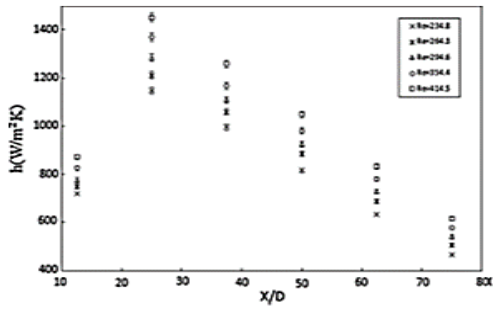
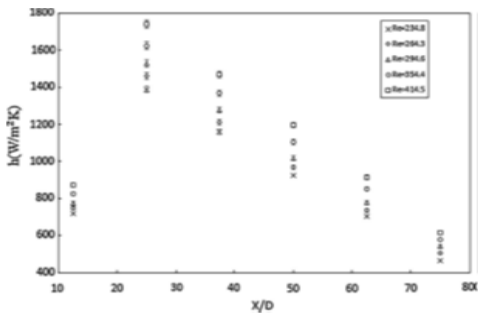


**Figure 13.** Length of the heat exchanger for different product inlet temperatures [26]

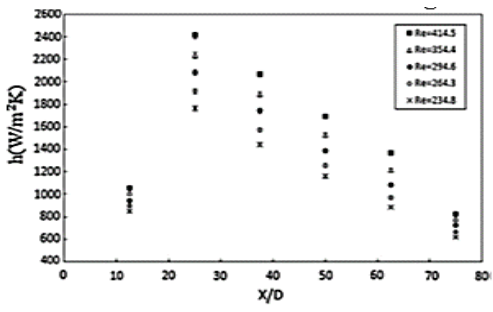


(a)

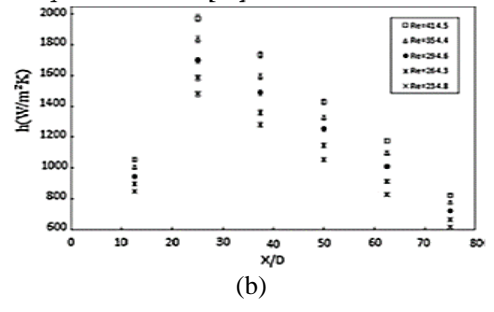


(b)

**Figure 14.** Heat transfer coefficient of distilled water in the non-magnetizable and magnetizable porous medium [27]

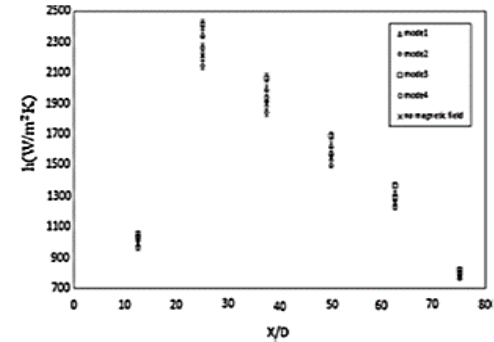


(a)

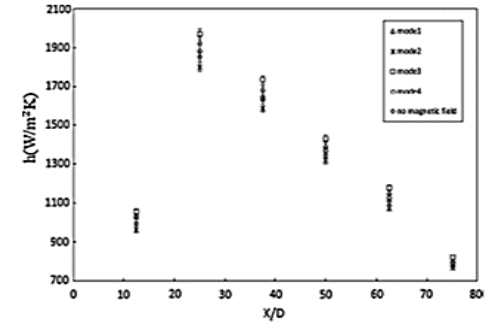


(b)

**Figure 15.** Effect of Reynolds number on the heat transfer coefficient of Ferro fluid in the magnetizable porous medium and non-magnetizable porous medium at  $f=10$  Hz and mode 3 [27]



(a)



(b)

**Figure 16.** Heat transfer coefficient of Ferro fluid 1.5% at different mode with  $f=10$  Hz in the magnetizable porous medium and non-magnetizable porous medium [27]

The heat transmission of Ferro fluid in magnetizable and non-magnetizable porous media under constant and fluctuating magnetic fields was researched, and the following results were obtained: As the volume % of nanoparticles and Reynolds number increase, the heat transfer coefficient of Ferro fluid improves. In order to explore the effect of porous media on the heat transfer coefficient, researchers looked at the flow of distilled water in non-magnetizable and magnetizable porous media, as well as the effects of Reynolds number on the heat transfer coefficient in porous media. The main purpose of these experiments was to see how porous media magnetization affected the heat transfer coefficient of Ferro fluid. These findings are depicted in Figures 14, 15, and 16 [27].

Changes in hydrodynamic characteristics, improved heat transmission through porous media in the channel, and pressure drop caused by porous media are all taken into account. It was discovered that increasing the width of a porous media and increasing the air flow rate can result in higher heat transfer rates. As the temperature rises, the temperature difference between the channel wall and the

fluid's average temperature decreases. Heat transfer coefficient is also increased by increasing the Reynolds number in all places of the porous material. The relevance of utilizing porous materials in increasing heat transmission is clearly highlighted in Figures 17, 18, 19, 20, as well as a higher value for heat transfer rates can be achieved [28].

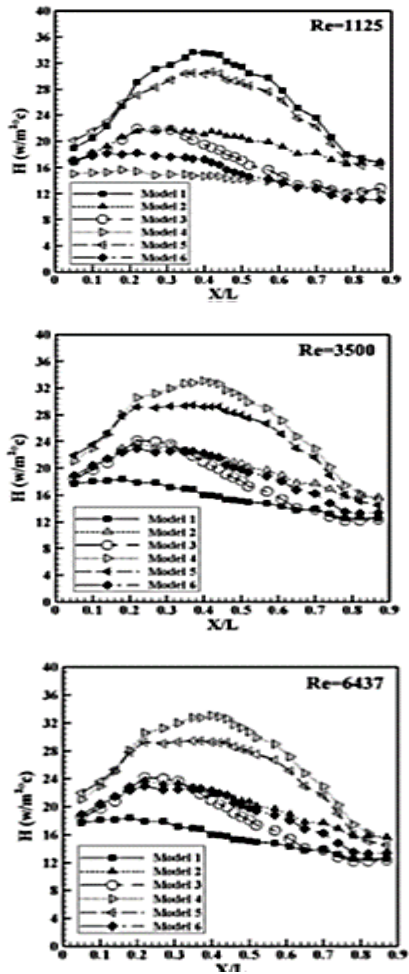


**Figure 17.** Convection heat transfer coefficient of all models at fixed heat flux ( $Q=275W$ ) for different Reynolds number ( $Re=1125,3500$  and  $6437$ ) [28]

In a tube with porous media, an experimental research of air mist flow is carried out. The porous region under investigation has a unique shape. The effect of operating parameters such as Reynolds number is also investigated. The following are the outcomes: The results demonstrate that the average Nusselt number augmentation is more than 200% at low Reynolds numbers. In the transient flow regime, heat transfer augmentation ranges from 100 to 265% for all models. At high Reynolds numbers, the best thermal performance improvement based on employing porous zone and mist flow is 467.7% heat transfer augmentation. Table 1 shows the size and shape of the porous media employed and the researched models (1). The value of employing (Figures 21-23) is clearly demonstrated [29].

The efficacy of a double-tube counter flow heat exchanger in porous media was investigated in an experimental investigation. Heat transport was aided by the porous aluminum plate medium used throughout the experiment, which had a large contact surface with the fluid and a high thermal conductivity. When a porous tube surface is employed, the amplification coefficient increases considerably. Using a single plate had a minor impact on the heat transfer coefficient,

however using three plates resulted in the best heat transfer coefficient (up to 35%). The relevance of employing porous materials in increasing heat transmission is clearly highlighted in Figures 24-26, and we note the heat transfer coefficient vs volume flow rate with varying mass concentrations of Nano fluid under the three-panel diagram [30].

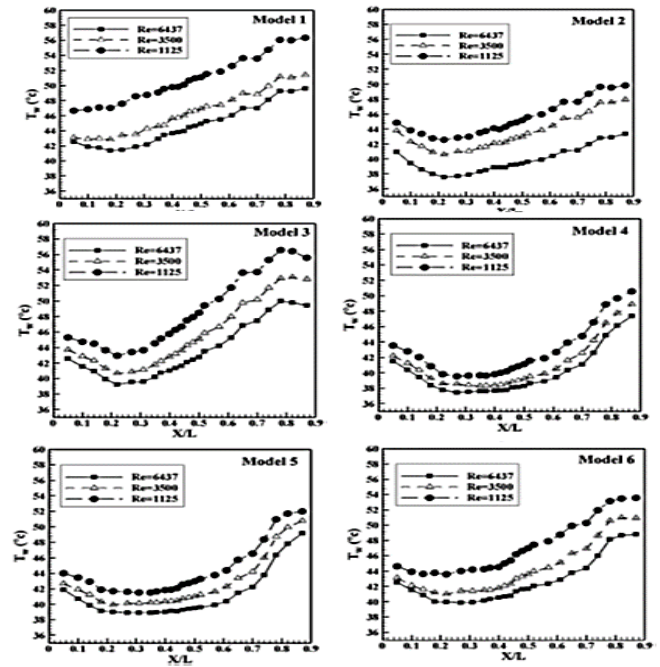


**Figure 18.** Temperature of channels wall for different model at fixed heavy flux ( $Q=275W$ ) for different Reynolds number [28]

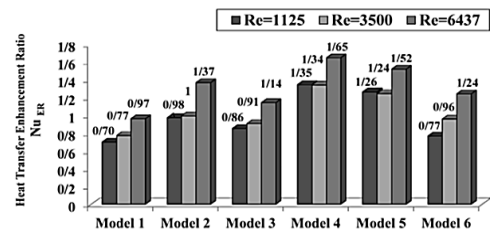


**Figure 19.** Heat transfer enhancement ratio for different models and different Reynolds numbers [28]

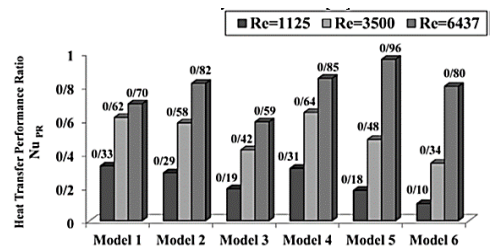


**Figure 20.** Heat transfer performance ratio ( $Nu_{PR}$ ) for different models and different Reynolds numbers [28]

**Table 1.** Dimensions of the porous media

Model	d (cm)	D (cm)
Model 1	0	4
Model 2	0	6
Model 3	0	8
Model 4	0	10
Model 5	2	10
Model 6	4	10

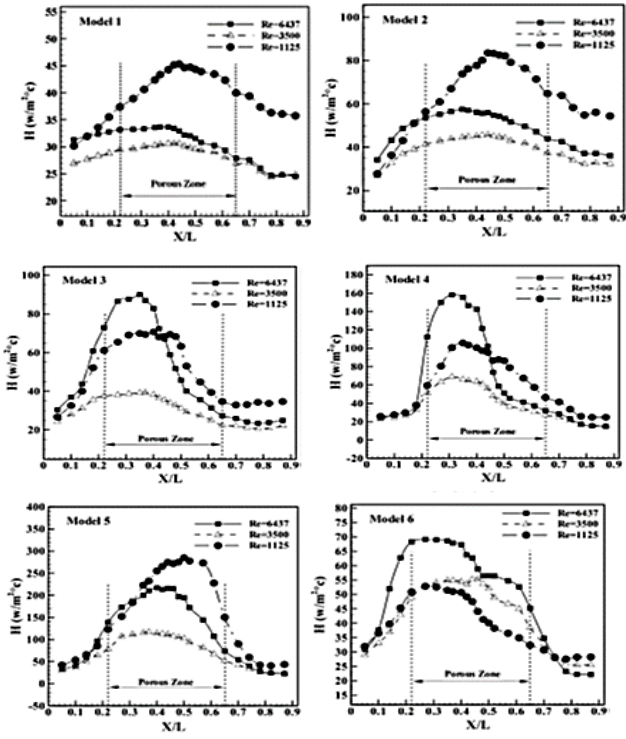


**Figure 21.** Effect of porous media in mist flow of heat transfer enhancement for all models at laminar flow ( $Q=275W$ ) for different Reynolds number ( $Re=1125$ ) [29]

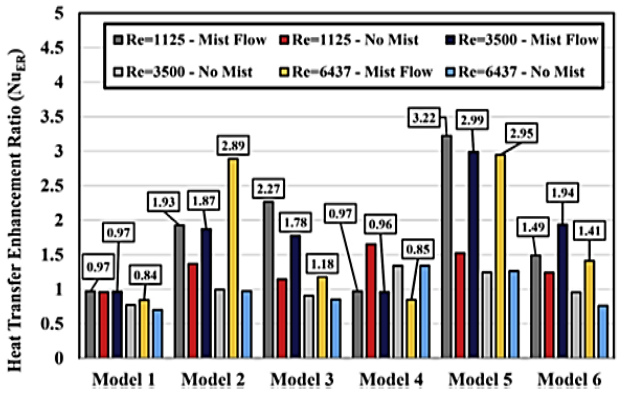


**Figure 22.** Heat transfer enhancement ratio for different models (mist flow and no mist flow) and different Reynolds numbers ( $Re=1125, 3500$  and  $6437$ ) [29]

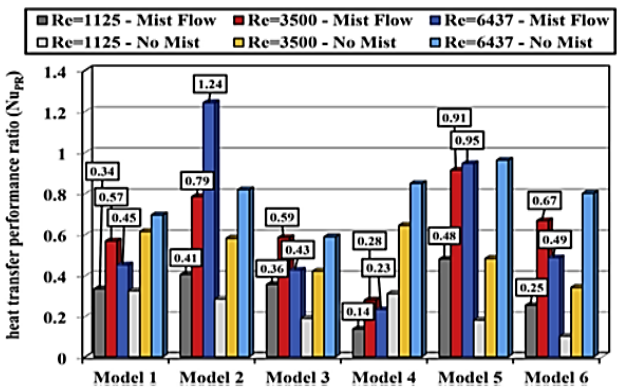


**Figure 23.** Heat transfer performance ratio ( $Nu_{PR}$ ) for different models and different Reynolds numbers [29]

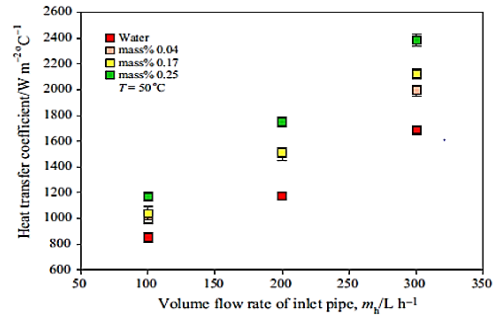


**Figure 24.** Heat transfer coefficient versus volume flow rate of inlet pipe at different mass concentration of nanofluid at temperature of  $50^{\circ}C$

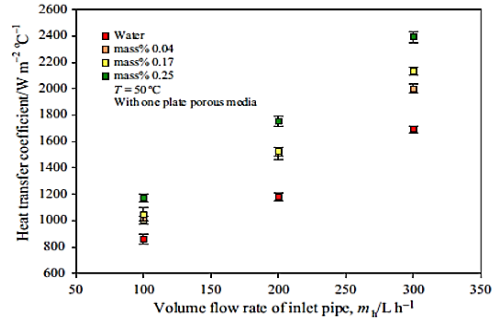


**Figure 25.** Heat transfer coefficient versus volume flow rate of inlet pipe at different mass concentration of nanofluid under one-plate porous media [30]

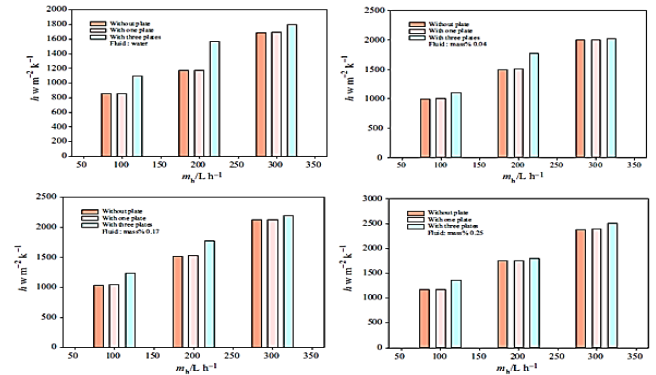


**Figure 26.** Heat transfer coefficient versus volume flow rate under different conditions [30]

The influence of enclosure size in latent heat thermal energy storage systems embedded in a porous medium for domestic use of latent heat thermal energy storage heat exchangers is examined in order to elucidate the effect of the specified media. The use of the porous-PCM storage technology resulted in an increase in heat transfer rate. The effect, however, is dependent on the storage unit's size. When the thermal diffusivity of the PCM solid-phase zone increases by almost 2.5 times that of the PCM alone, a stronger effect of the porous media on the melting process is observed. Furthermore, the impact of porous media on melting time is strongly linked to the storage system's aspect ratio (width to height). The relevance of employing porous materials in enhancing heat transfer is clearly illustrated in Figures 27-32, and we also note its effect on the dissolving process, since the time necessary to complete the dissolution process lowers [31].

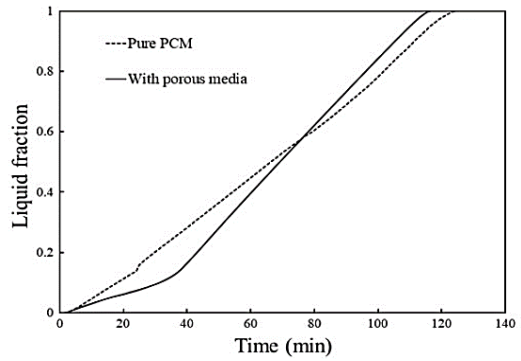


**Figure 27.** The mean liquid fraction at different time for both PCM-only and porous PCM cases [31]

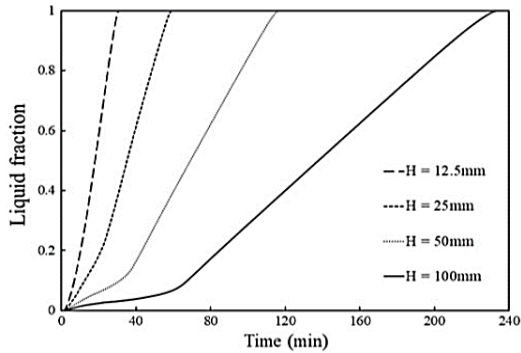


**Figure 28.** Mean liquid fraction at different time for porous-PCM for various heights of the storage system [31]

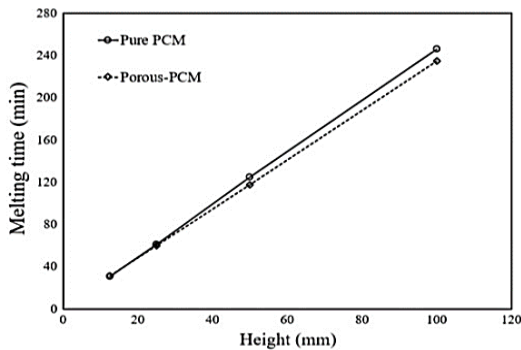


**Figure 29.** The effect of system height on the melting time for a constant induced heat flux for both systems of PCM-only and porous-PCM [31]

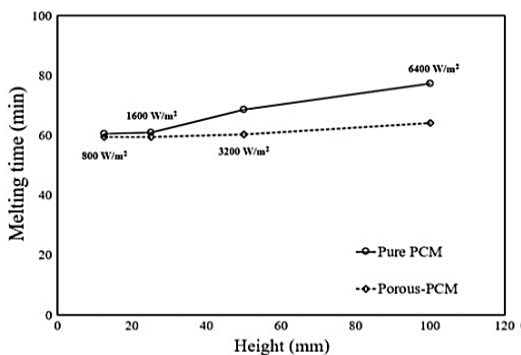


**Figure 30.** The effect of system height on the melting time for various induced heat flux regarding Table 1 for both cases of CM-only and porous-PCM [31]

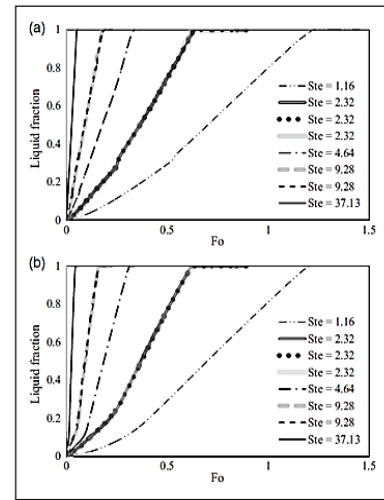


**Figure 31.** The variation of liquid fraction as a function of Fourier number for different Stefan number for LHTES system with (a) PCM-only and (b) composite-PCM [31]

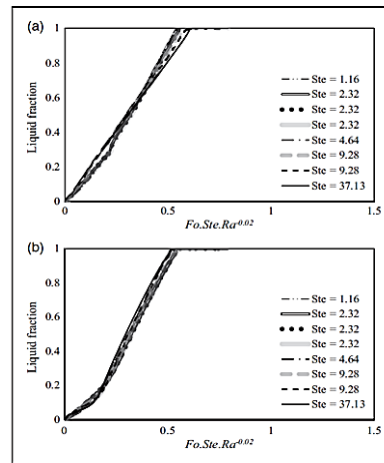


**Figure 32.** The variation of liquid fraction in terms of  $Fo \cdot Ste \cdot Ra^{0.02}$  for LHTES system with (a) PCM-only and (b) composite-PCM [31]

In addition to facilitating heat transfer, porous material can also increase pressure drop. The magneto hydrodynamics forced convection effects of  $Al_2O_3$ -CuO-water Nanofluid inside a partitioned cylinder within a porous medium are investigated numerically. The maximum PEC in the examined Nanofluid was obtained by increasing the magnetic field orientation to a specified value ( $90^\circ$ ) [32] as shown in Figures 33-36. The thermal efficiency of the modified Trombe-wall system proposed in this work is improved over its original counterpart because a porous substance is incorporated to the absorber wall. Natural convective heat transfer in the revised active cavity of the Trombe-wall system is increased by around 4% to 23% on average, according to the Rayleigh number utilized in this study. This enhances the total thermal efficiency of the new version suggested here, which was achieved through a simple and easy-to-implement change based on the addition of a conductive porous material layer [33]. The goal of this project is to undertake a 3D numerical study of the laminar flow and heat transfer of an  $Al_2O_3$  - CuO - water hybrid Nano fluid inside a U-bend pipe in a porous material. The Darcy number could be increased to improve the PEC. In all cases of Nano fluids, increasing the volume percentage of nanoparticles (from 0% to 5%) increased the

mean Nusselt number and pressure drop, whereas the PEC showed a falling pattern. Metal nanoparticles incorporated into the base fluid may improve the average heat transfer coefficient and averaged Nusselt number. The importance of porous materials in enhancing heat transfer was clearly demonstrated in Figures 40-45, as we can see from the improved heat transmission, the average Nusselt number increased and the pressure reduced, while the PEC displayed a declining trend. Metal nanoparticles incorporated into the base fluid can improve the average heat transfer coefficient and Nusselt number [34].

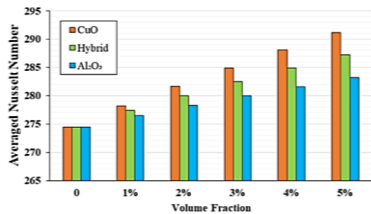


**Figure 33.** Comparison of averaged Nusselt number for different volume fraction in three case of Al<sub>2</sub>O<sub>3</sub>, CuO and hybrid Nano fluid [34]

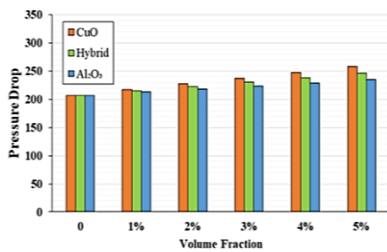


**Figure 34.** Comparison of pressure drop for different volume fraction in three cases of Al<sub>2</sub>O<sub>3</sub>, CuO and hybrid Nano fluid [34]

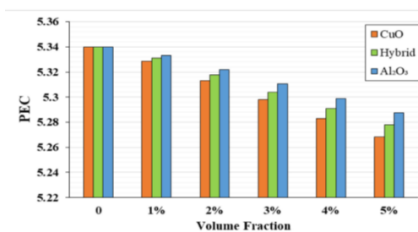


**Figure 35.** Comparison of PEC for different volume fraction in three cases of Al<sub>2</sub>O<sub>3</sub>, CuO and hybrid Nano fluid [34]

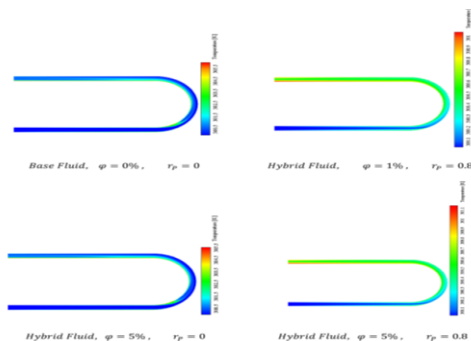


**Figure 36.** Temperature contours for different volume fractions using water as base fluid and hybrid Nano fluid [34]

At Richardson numbers (Ri) of 0.01, 10, and 100 (and Darcy numbers (Da) of 10-4 Da 10-2), a mixed flow of non-

Newtonian water/Al<sub>2</sub>O<sub>3</sub> Nanofluid with 0–4 percent nanoparticle volume fractions inside a two-dimensional square cavity with hot and cold lid-driven motion and porous medium is simulated. The volume % of cooling Nanofluid used, as well as fluid direction penetrability (Darcy number), are important elements that influence streamline behavior. Due to the greater forced motion characteristics of fluid, the Richardson number is reduced. Higher velocity gradients result from changing the nanoparticle volume fraction and Darcy number, resulting in considerable changes in streamline pattern [35]. Heat transmission through convection in porous medium is a common occurrence in science and engineering, as well as a natural phenomenon. At the representative elementary volume (REV) scale, this work provides a cascaded lattice Boltzmann (CLB) approach for convective heat transfer in porous media. In the CLB technique, a temperature-based CLB model with the D2Q5 lattice solves the temperature field, while an isothermal CLB model based on the extended non-Darcy model with the D2Q9 lattice solves the flow field. Indicate that the existing CLB technique may be utilized to perform large-scale engineering computations of convective heat transfer in porous media in an efficient and powerful manner [36]. The heating of wood pellets in a batch reactor using hot exhaust fumes from an engine is investigated in this work. Over time, the temperature and velocity of hot gases entering the reactor were measured. A first test was conducted with 15 percent sawdust hemisphere pellets, followed by a second test using carbonized pellets from the first. Carbonized pellets, which are virtually inert, have a lower thermal capacity and a less uniform heating pattern than fresh pellets. The energy released by the exhaust passing through the biomass was calculated as the total of the energy absorbed by the pellets and the thermal losses. The findings of this investigation are shown in Figures 37, 38 [37].

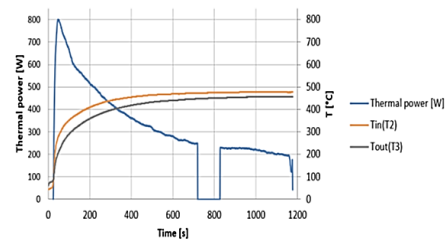


**Figure 37.** Thermal power vs inlet and outlet temperature, during the second test [37]

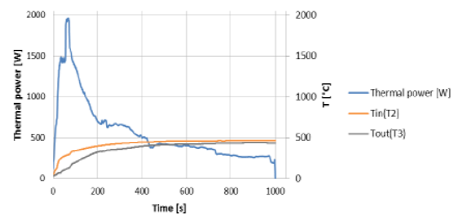


**Figure 38.** Thermal power vs inlet and outlet temperature, during the first test [37]

Using recently designed active-distributed temperature sensing experiments, groundwater fluxes emerging from heterogeneous flow fields may now be detected directly. Based on fundamental concepts and numerical simulations, two interpretation approaches for active-distributed temperature sensing experiments are presented here to estimate both the porous media thermal conductivities and

groundwater flows in sediments. By determining the duration of the conduction-dominant stage, the effective thermal conductivity of the media may be easily established, regardless of groundwater flow (by graphically estimating the slope of the temperature increase during this stage and or by reproducing the temperature rise using the MILS model). The temperature change caused by heat transfer in porous medium may then be efficiently predicted using the MILS analytical method to produce reliable groundwater flux estimations. In addition, a graphical study of the thermal response curves recorded along the wire can provide an accurate and independent estimation [38]. The discrete unified gas-kinetic scheme (DUGKS) is extended to convective heat transport in porous media at the representative elementary volume (REV) scale, with two kinetic equations describing changes in velocity and temperature fields. The effects of the porous medium are incorporated into the technique by incorporating porosity in the equilibrium distribution function and adding a resistance force to the kinetic equation for the velocity field. By including the impacts of porous media into the equilibrium distribution function and adding the flow resistance force to the kinetic equation for velocity field, the effects of porous media are taken into account. The current model is more numerically stable. Additionally, non-uniform meshes can be used to boost computational efficiency [39]. In tropical locations, some cooling technologies, such as fluid flows, phase change materials (PCMs), and porous media, have been advocated as viable options. In this study, these tactics are combined experimentally to create a new low-cost porous medium by improving the thermal conductivity of the phase transition material with aluminum shavings, which are considered waste materials in some industries.

PV/T-PCM-Porous produced the highest electrical power while having the lowest PV panel temperature. At midday in July, the PV temperature reduced by 36.5% when compared to the solo PV unit, but the electrical power increased by 17.7%. In December, the reduction in PV temperature and increase in electrical power were 33.2% and 14.2%, respectively. The use of aluminum shavings in the PCM could have three favorable effects: a more consistent temperature profile, a 19% to 25% reduction in melting time, and a faster transfer of heat from the dissipated heat to the water channels. Some of the findings of this investigation are shown in (Figures 39, 40) [40].

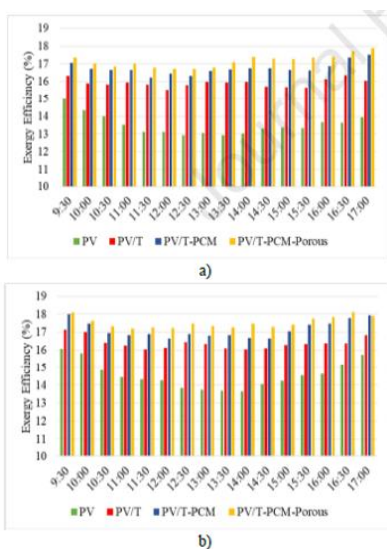


**Figure 39.** Exergy efficiency during hour of the test day (a) warm month (b) cold month [40]

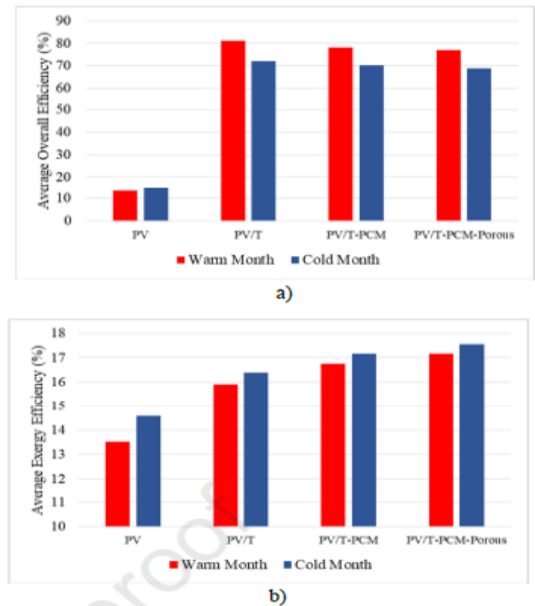


**Figure 40.** Average efficiency of the cases (a) overall efficiency (b) exergy efficiency [40]

This research uses the thermophysical features of Nanofluid saturated porous media to improve the thermal design of a spherical electronic device. Furthermore, the ratio of the thermal conductivity of the porous material's matrix to that of the base fluid (water) has a substantial impact on heat transmission across the entire fraction volume treated range [41].

#### 4. IMPROVE HEAT TRANSFER BY NANOFLUID

For the purpose of improving heat transfer and maximizing energy utilization, Nanofluid are used as an inexpensive way to extend the heat transfer area, and improve effective thermal conductivity. On an automotive flat tube plain fin compact heat exchanger, experiments were done utilizing ethylene glycol as a base fluid, diamond and SiO<sub>2</sub> as coolants, and nanoparticle volume fractions ( ) ranging from 0.1 percent to 2 percent. When the particle volume percentage of a Compact Heat Exchanger using Nanofluid increased, the thermal performance improved significantly. The importance of employing Nanofluid in increasing heat transfer was clearly demonstrated in Figures 41, 42, as this study also discovered that heat transfer coefficient increases linearly as particle volume fraction increases [42].

The thermal conductivity of base fluids is known to increase when colloidal particles are present. The form and structure of the solid particles have a significant impact on the extent of amplification. The lowest increase is produced by spherical particles, the only form for which analytic theories exist. Spherical particles have the lowest possible thermal conductivity at given volume fractions. In comparison to completely scattered spheres, structures generated by generating connections between primary particles always have better conductivity. The value of utilizing Nanofluid in increasing heat transmission was clearly demonstrated in Figures 43, 44, as the structures encasing the fluid in locations that are thermally separated from the main fluid improved the most. A robust spherical shell filled with suspension fluid is excellent [43].

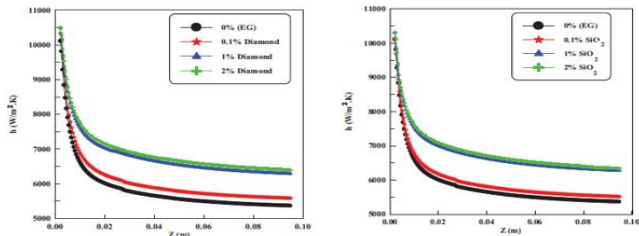


**Figure 41.** Variation of heat transfer coefficient along the tube length for diamond and SiO<sub>2</sub> with different volume fractions [42]

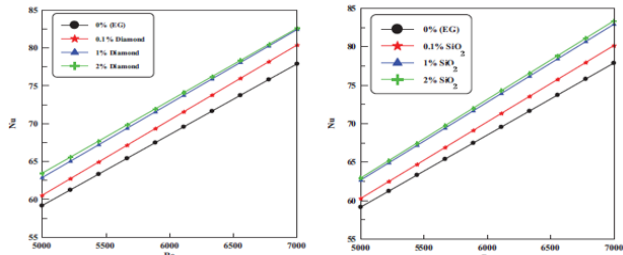


**Figure 42.** Variation of average coolant Nusselt number against the coolant Reynolds number for diamond and SiO<sub>2</sub> with different volume fractions [42]

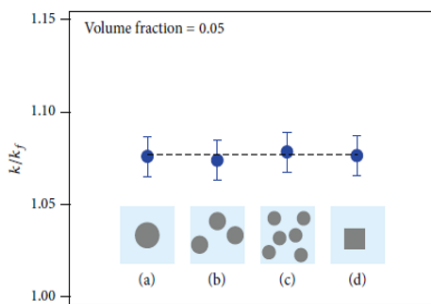


**Figure 43.** Effect of particle size of spherical particles with  $k_p/k_f$  [43]

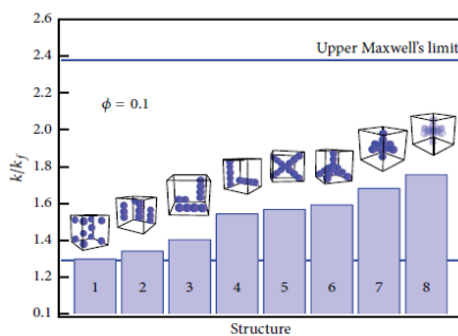


**Figure 44.** Effect of aggregation state and cluster configuration on conductivity enhancement [43]

Heat transfer rate augmentation in the vehicle cooling system is the subject of an experimental investigation. Nanofluid is made by suspending nanoparticles in a liquid foundation. Suspension of Nanofluid in a base fluid completely modifies the characteristics of the base fluid, resulting in a fluid with improved performance. In this article, a comparison of TiO<sub>2</sub>-W and SiO<sub>2</sub>-W is made. In the automobile cooling system, Nanofluid is employed to improve heat transfer rate. The rate of heat transmission is related to the

Reynolds number. As the volume concentration rises, so does the pressure decrease? The heat transmission rate of spherical nanomaterials is higher than that of other forms. Because nanoparticles have a small surface area per unit volume, the heat transmission rate decreases as their size increases [44]. The influence of curves connected to thermosiphons and heat pipes with varying active fluids and inclination angles on thermal efficiency was investigated experimentally. The Nanofluid used in this study is an aqueous solubility in pure water of Al<sub>2</sub>O<sub>3</sub> nanoparticles with a diameter of 35 nanometers. The test saturation levels for nanoparticles are 0%, 1%, and 3% by weight. All of the studies were carried out and repeated at 30°, 60°, and 90° inclination angles (vertical). The value of utilizing Nanofluid in boosting heat transmission was clearly demonstrated in Figures 45-48, as the thermal efficiency of heat pipes improves with increasing nanoparticle concentrations and tilt angles [45].

Experimental analysis is used to explore the hydrothermal behavior of a refrigerant-based Nanofluid (Nano-refrigerant) during condensation within a horizontal tube.

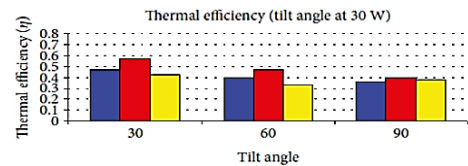


**Figure 45.** Alteration of thermal efficiency of heat pipes by various tilt angles and fluids of heat pipes at 30W power [45]

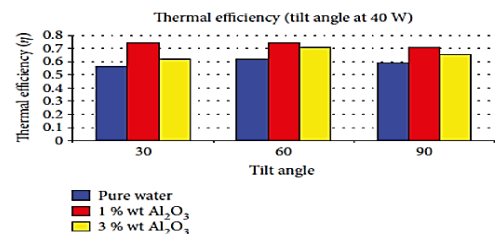


**Figure 46.** Alteration of thermal efficiency of heat pipes by various tilt angles and fluids of heat pipes at 40W power [45]

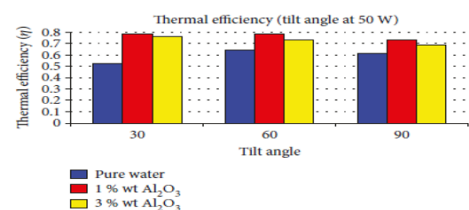


**Figure 47.** Alteration of thermal efficiency of heat pipes by various tilt angles and fluids of heat pipes at 50W power [45]

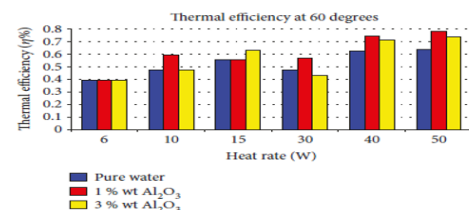


**Figure 48.** Variations of thermal efficiency in different heat rate at 60° tilt [45]

To manufacture Nano refrigerant, R600a and CuO are utilized as the base fluid and nanoparticle, respectively. Nanofluid mass fractions (0.5, 1%, and 1.5%), mass fluxes (154.6 to 265.4 kg m<sup>-2</sup>s<sup>-1</sup>), and vapor quality (0.1 to 0.8) are all investigated. Lower vapor quality and low mass fluxes create higher PEC values, whereas higher nanoparticle concentrations produce larger PEC values. It was also shown that increasing the nanoparticle concentration resulted in a

greater frictional pressure drop of Nano refrigerant compared to the baseline combination. The relevance of utilizing Nanofluid in increasing heat transfer was clearly demonstrated in Figures 49, 50, as the Nano cooler has a higher friction pressure drop than the baseline mixture, and the higher the nanoparticle concentration, the higher the friction pressure drop [46].

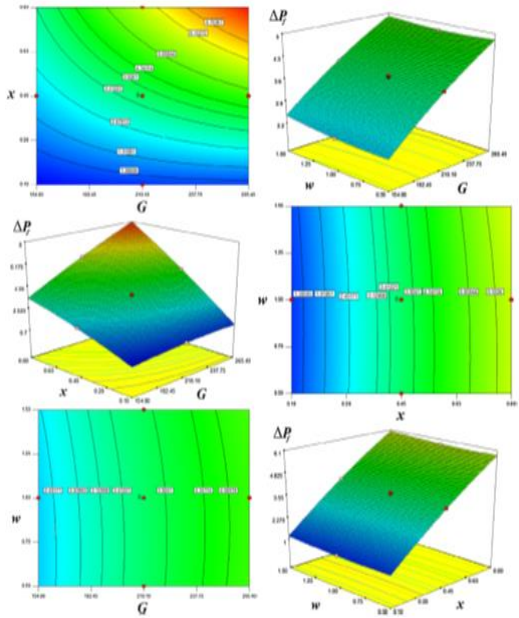


**Figure 49.** Effects of mass flux, vapor quality, and mass fraction of nanoparticles on pressure drop [46]

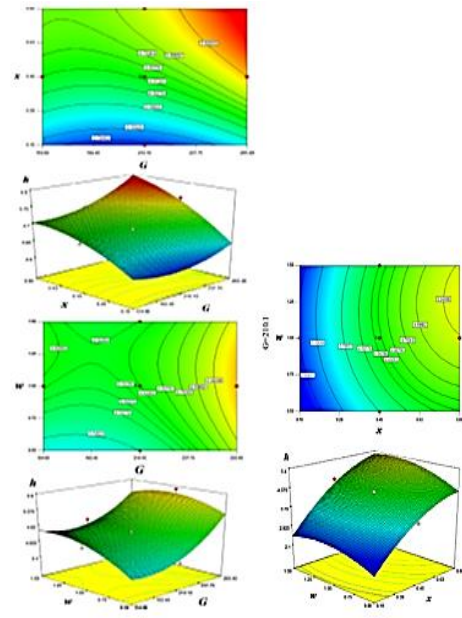


**Figure 50.** Effects of mass flux, vapor quality, and mass fraction of nanoparticles on condensation heat transfer coefficient [46]

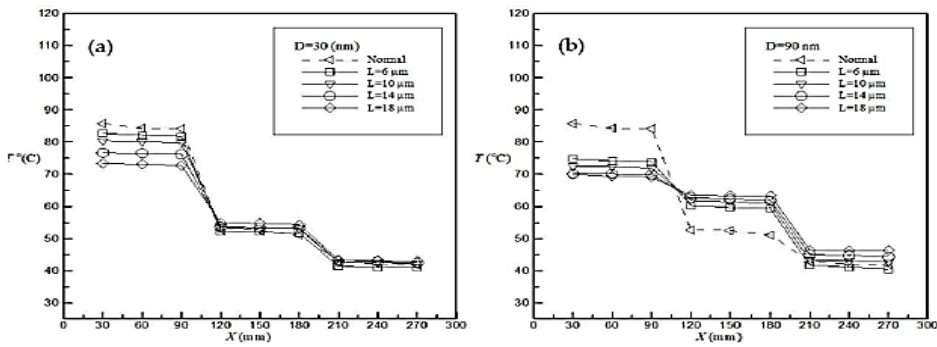


**Figure 51.** Temperature distribution along heat pipe at  $Q_{in}=100$  W for different values of the tube length  $L$  with:  $D=30, 90$  nm [47]

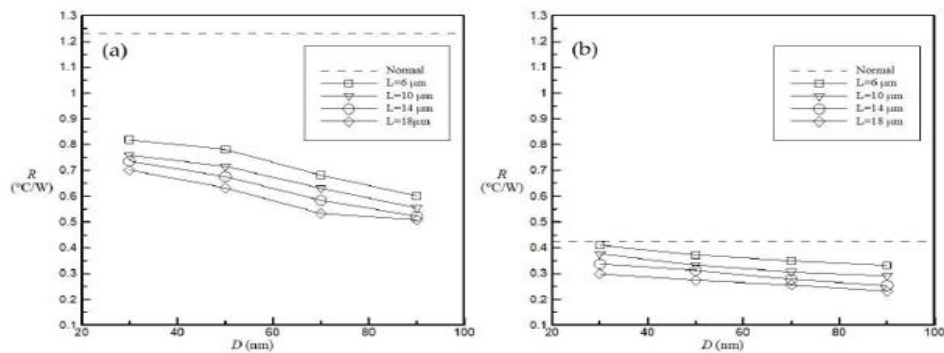


**Figure 52.** Variation of the overall thermal resistance  $R$  with the tube diameter  $D$  for different values of the tube length  $L$  with:  $Q_{in}=25$  W, 100 W [47]

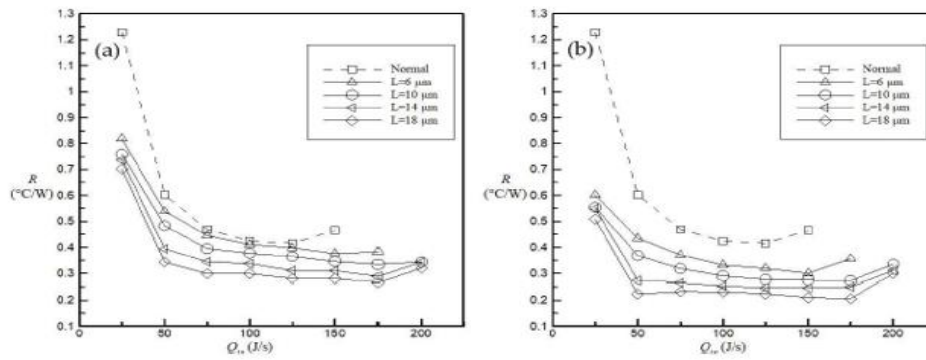


**Figure 53.** Variation of the overall thermal resistance  $R$  with the input heat power  $Q$  in for different values of the tube length  $L$  with:  $D=30,90$  nm [47]

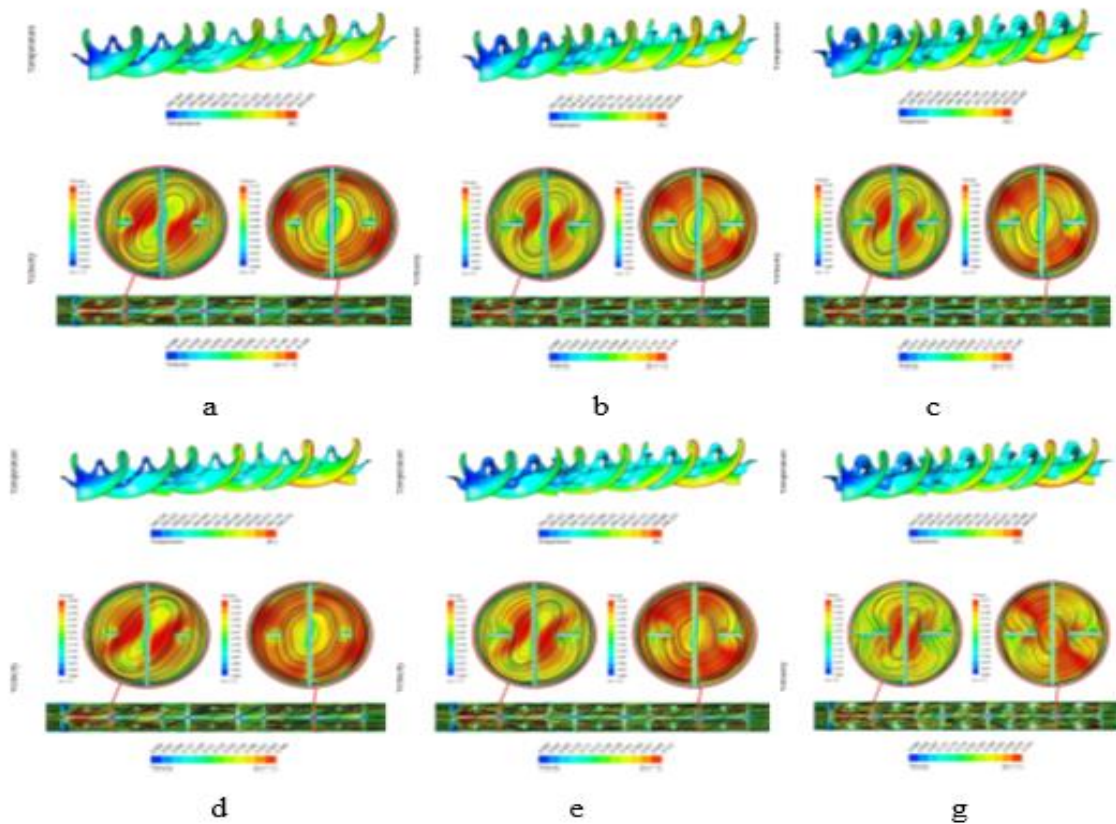


**Figure 54.** Distribution of temperature and velocity when (a, b, c) ( $b=5, 10, 15$  mm),  $Re=5000$ , (d, e, g) ( $b=5, 10, 15$  mm),  $Re=15000$  [48]

The main goal is to look into how the length and diameter of anodic aluminum oxide nanotubes affect temperature distribution and overall thermal resistance. By increasing the length and diameter of anodic aluminum oxide nanotubes, the temperature difference between the evaporator and condenser sections may be reduced. The value of Nanofluid in increasing heat transfer was clearly demonstrated in Figures 51-53, where the maximum applicable input heat energy to avoid dehydration can be enhanced by up to 40% when compared to an untreated heat pipe. As the input heat energy  $Q_{in}$  grows, we reduce the overall thermal resistance  $R$  [47].

The Finite volume approach was utilized to demonstrate the nanomaterial hydrothermal behavior within a duct, and a helical complex device was added to increase the performance. Any insert used inside a pipe can cause tangential velocity to increase and the temperature boundary layer to thin. Nanofluid flow can have a faster velocity when the device width is raised,

making it more apparent near the heated surface. In Figure 54, secondary flow has a major impact on axial velocity, and flow resistance increases as swirl flow becomes more powerful [48].

The current study shows turbulent nanofluid flow inside a solar collector. With the addition of a new turbolentor, turbulence mixing has been improved. Within the test tube equipped with multichannel twisted tape components, heat transmission and exergy behavior were studied. Inside the pipe, an  $Al_2O_3$ -water nanofluid circulates. Aluminum is used to make absorber plates. The effects of key variables on exergy loss and second-law efficiency have been addressed. Exergy loss tends to decrease as the number of revolutions and channels increases. Increasing the diameter ratio improves the effectiveness of the second law [49].

To achieve superior thermal performance, a combined turbolentor was proposed. The k-e model was used to simulate a steady turbulent flow of copper oxide nanofluid using a

homogeneous model. Disturbance of the boundary layer is a critical aspect in improving heat transmission. The improved thermal management may be achieved by using a higher height. Lowering  $b$  weakens the boundary layer by causing fluid mixing and disruption. The fluctuation of  $X_d$  as a function of  $Re$  and  $b$  is shown in Figure 55-56. Higher levels of  $Re$  and  $b$  have been linked to more intense disturbance and nanofluid fluid mixing [50].

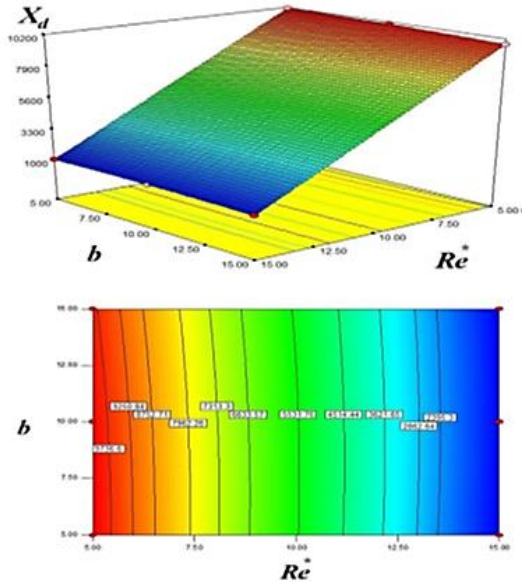


Figure 55. Exergy loss for different values of  $Re$  and  $b$  [50]

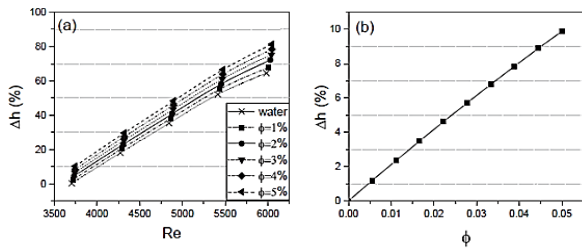


Figure 56. (a) Effect of nanofluid Reynolds number on heat transfer coefficient relative change,  $\Delta h(\%)$ , and (b) variation of  $\Delta h(\%)$  for various nanoparticle volume fractions and  $Re=3700$  [51]

This paper describes the usage of an  $Al_2O_3$ -water Nanofluid as a precooler for  $SCO_2$  Brayton cycles. Because the precooler plays such an important role in total performance, choosing the right working fluid is crucial. The precooled thermal-hydraulic parameters were predicted using a segmental analysis, which led to the use of a printed-circuit heat exchanger. The nanoparticle volume percent in the range of 0–5% affects the thermal conductivity, heat transfer coefficient, and total heat exchanger length. It has been demonstrated that as the volume fraction increases, the heat transfer improves by 10%. Finally, when compared to pure water, the pressure drop of the heat exchanger was reduced by up to 14% for  $\phi = 5$  percent, which could have a significant impact on whole cycle efficiency. Influence of Nanofluid Reynolds number on heat transfer coefficient relative change, effect of nanoparticle volume percent on heat exchanger length change, and friction factor variation as nanoparticle volume fraction are shown in Figure 57, 58 [51].

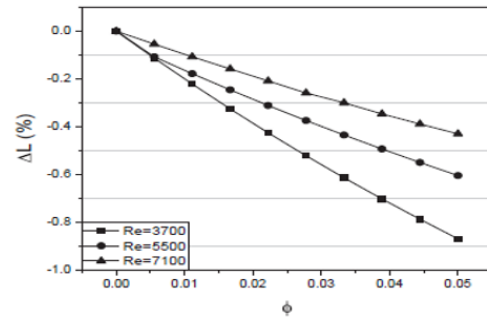


Figure 57. Effect of the nanoparticle volume fraction on the heat exchanger length change for  $Re=3700, 5500$  and  $7100$  [51]

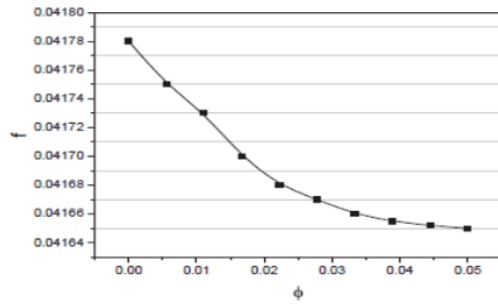


Figure 58. Friction factor variation as the nanoparticle volume fraction increases [51]

In this case, a two-phase technique was used to investigate the treatment of Nanofluid within a thermal unit fitted with a turbolentor. Helical tape (case I), Barrier helical tape (case II), and Perforated Barrier helical tape (case III) were used (Case III). In compared to the first example, the second case design has a greater radial flow, which results in higher residence time and a lower temperature gradient. Furthermore, when the turbolentor style changes from Case II to Case III, the quantity of  $X_d$  increases by about 8.87 percent and 5.7 percent for the lowest and highest pumping power, respectively. Show findings for Nusselt number, pressure, and  $X_d$  for various scenarios in Figures 59-61 [52].

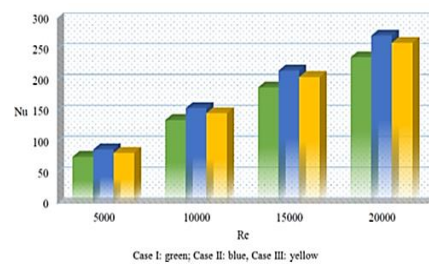


Figure 59. Nu values for different cases [52]

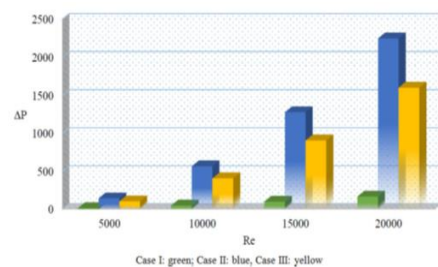


Figure 60.  $\Delta P$  values for different cases [52]

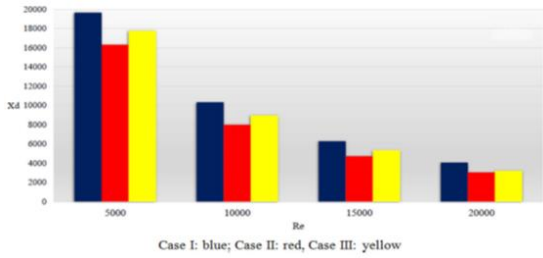


Figure 61.  $X_d$  values for different cases [52]

Multi tapes were used in this case to increase the productivity of the thermal unit, which was loaded with hybrid Nano powder. The k-approach was used to evaluate turbulent flow, and FVM was used to solve the governing equations, using two formulae for Nu and friction factor in outputs. The addition of a swirl flow device causes the nanomaterial to make greater contact with the wall, increasing pressure drop and Nusselt number. According to the results, raising Re causes a larger pressure drop as well as a higher bulk velocity. While pressure loss rises, more turbulence intensity may be seen with the help of the thermal performance. The influence of N on Nu decreases by around 7.14 percent at the greatest Re. At  $Re^* = 5$ , increasing N causes a 13.58 percent and 55.28 percent increase in velocity and pressure, respectively. Show findings for Hydrothermal Behavior of Nanomaterials and Corresponding Numerical Values in Figures 62, 63 [53].

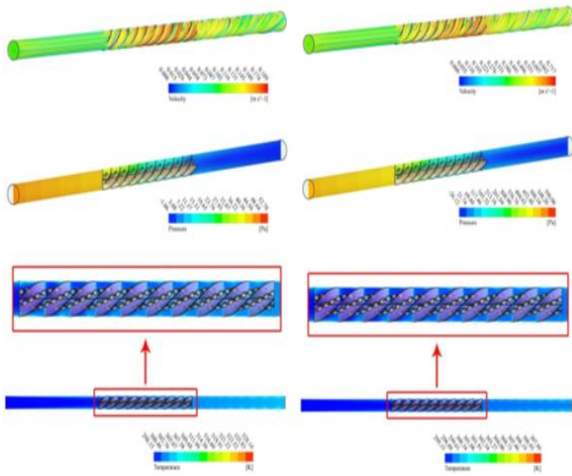


Figure 62. Hydrothermal behavior of nanomaterial when  $N=2.5$ , ( $Re=5000, 20000$ ) [53]

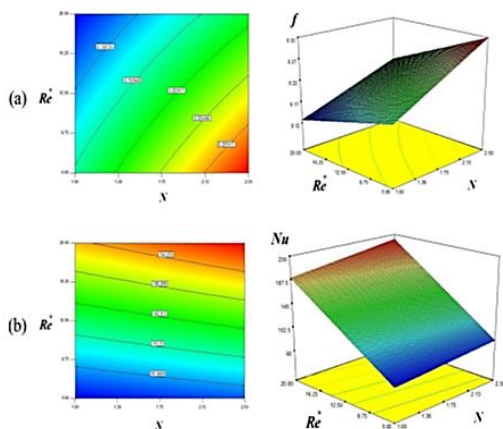


Figure 63. Corresponding values of Nu and f with changing N and Re [53]

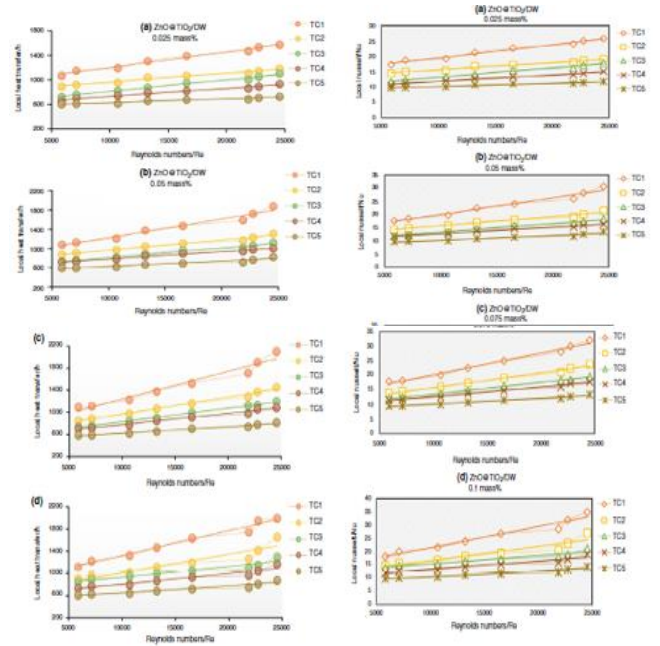
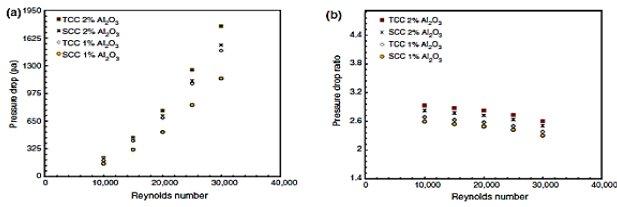


Figure 64. Variations in a local heat transfer calculation and Improvement in: (a) local Nusselt numbers for 0.025 mass % and (b) local heat transfer calculations for 0.05 mass %, (c) local heat transfer calculations for 0.075 mass % and (d) local heat transfer calculations for 0.01 mass %, of ZnO @ TiO<sub>2</sub>/DW-based nanofluid [54]

The concentrations of ZnO@TiO<sub>2</sub>/DW binary composite nanofluid (0.1, 0.075, 0.05, and 0.025 mass percent) have been considered. To create binary composite nanofluid, ZnO was manufactured using a simple single-pot son chemical technique and combined with TiO<sub>2</sub> under high probe sonication. The effective thermal conductivity experiment was carried out at temperatures ranging from 20 to 45 degrees Celsius. The 50:50 mass ratio of ZnO and TiO<sub>2</sub> nanoparticles is the best combination for achieving efficient thermal conductivity. The 0.1 mass percent concentration of ZnO@TiO<sub>2</sub>/DW binary composite nanofluid is expected to characterize the binary composite nanofluid's higher thermal performances based on thermophysical characteristics and rendering to the Reynolds range of 5849 to 24,544. At the several tested circumstances, the 0.1 mass percent showed the greatest improvement in average heat transfer of ZnO@TiO<sub>2</sub>/DW binary composite nanofluid. Some of the findings of this investigation are depicted in Figure 64 [54].

The effects of coupled corrugated walls and turbulent Nanofluid flow on thermo-hydraulic performance in corrugated channels are compared throughout Reynolds number ranges of 10,000–30,000 and constant heat flux of 1 104 W m<sup>2</sup> in an experimental study. Three types of Al<sub>2</sub>O<sub>3</sub>–water nanofluid channels are created and tested using 1% and 2% volume fractions of Al<sub>2</sub>O<sub>3</sub>–water nanofluid: semicircle corrugated channel, trapezoidal corrugated channel (TCC), and straight channel. It was successful to prepare and test Al<sub>2</sub>O<sub>3</sub> nanoparticles suspended in water with two volume fractions () of 1.0 percent and 2.0 percent. The use of corrugated channels results in a noticeable increase in heat transmission, as well as a little rise in p. The kind of corrugation determines how well heat is transferred. The impact of the corrugation profile on heat transfer enhancement is greater than that of the nanofluid. Some of the findings of this investigation are shown in Figures 65, 66 [55].



**Figure 65.** Influence of Al<sub>2</sub>O<sub>3</sub>-water nanofluid volume fraction on pressure drop [55]

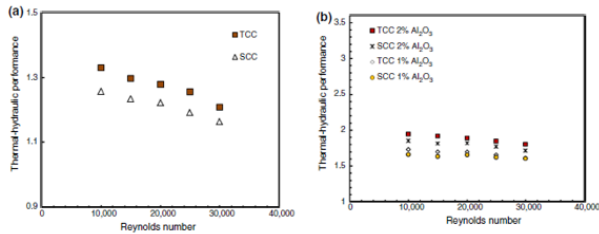


**Figure 66.** Influence of corrugated channels on thermal-hydraulic performance: a water and b Al<sub>2</sub>O<sub>3</sub>-water nanofluid [55]

The lattice Boltzmann technique was used to investigate the influence of electric field on the natural convective heat transfer enhancement mechanism of nanofluid (LBM). The forces of the electric field on nanoparticles were also discussed. Natural convection produces a velocity and temperature field, which is reformed by electric field forces. When compared to the velocity of the working medium, the velocity of nanoparticles is substantially lower, and the motion trends of nanoparticles and base fluid driven by an electric field are inverse [56]. The goal of this paper is to discuss advancements in obstacle surface design, heat transfer enhancement, and nanofluid flow performance in channels. The impacts of four different types of nanoparticles, each with a different concentration, particle diameter, and channel type. This article also discusses the key factors that influence the thermal performance of various shape channels with diverse obstacles and nanofluid flow. The addition of nanoparticles to the base fluid also improves the heat transmission properties significantly. Both analytical and experimental data in this research show that combining nanoparticles with base fluid improves heat transmission significantly. When water is substituted with nanofluid at a higher volume ratio, a high gradient in wall temperature occurs [57]. Given the slip situation, heat transport and entropy formation in a microchannel containing water nanofluid were explored. The use of injection method in the presence of a magnetic field was the major emphasis. The upper high-temperature wall injection was included into the flow field. Vortex formation is caused by a high Reynolds number, which limits local heat transmission in the neighboring zone. The vortex strength was reduced by using a magnetic field. The maximum heat transmission happens when the Hartmann and Reynolds numbers are the highest [58]. Experiments were conducted to investigate the hydrothermal properties of an Al<sub>2</sub>O<sub>3</sub> + TiO<sub>2</sub> hybrid Nanofluid flowing in a double-tube heat exchanger with various modified V-cuts twisted tape inserts under turbulent conditions. The hybrid Nanofluid is generated by dispersing Al<sub>2</sub>O<sub>3</sub> and TiO<sub>2</sub> nanoparticles in distilled water in an equal volume ratio, with a volume concentration of 0.1%. A decrease in twist ratio improves nu and f for the same

Reynolds number. Heat transfer and friction factor are improved the most with V-cuts twisted tape with a higher depth ratio and a lower width ratio. Nu and f climb as the Nanofluid inlet temperature is reduced at a given twist, depth, and breadth ratio. The nu enhancement of hybrid Nanofluid at 50°C is 13.57 percent higher than at 70°C, while the friction factor increases of hybrid Nanofluid at 50°C is 8.74 percent higher than at 70°C [59]. Different models were used to compare experimental data with the improvement in convective heat transfer and Nusselt number. The impacts of temperature dependency, temperature independence, and Brownian motion were examined using the models used. According to the Corcione and Maiga models, adding nanoparticles improves effective thermal conductivity, heat transfer coefficient, and effective dynamic viscosity to effective density, hence increasing the Nano fluid's velocity field. The Vajha model has a unique mechanism. The effective dynamic viscosity drops at a certain nanoparticle's ratio, reducing velocity, while the effective thermal conductivity improves sufficiently to enhance the Nano fluid's heat transfer coefficient with the addition of nanoparticles [60].

## 5. IMPROVE HEAT TRANSFER BY FINS

For the purpose of improving heat transfer and maximizing energy utilization, fins are used as an inexpensive way to extend the heat transfer area, and improve effective thermal conductivity. The design and operating parameters of a finned spiral heat exchanger were investigated experimentally in order to determine their impact on the performance of the MHV charging process. According to the experimental findings, including fins greatly decreases the MHV absorption/desorption times. Furthermore, the presented and obtained findings suggest that a correct choice of these parameters is critical for charge/discharge time management. The purpose of this experiment was to see how the copper fins affected the absorption process. Show the effect of the copper fins and the water temperature on the absorption process in Figures 67, 68 [61].

Experimentally, the thermal performance of a single pass solar air heater with five fins was examined. To promote heat exchange and make the flow fluid in the channel uniform, longitudinal fins were used inferior to the absorber plate. The efficiency of the collector increases with increased solar intensity due to improved heat transfer to the air flow at mass flow rates of 0.012 and 0.016 kg s<sup>-1</sup>. It has been proven that the solar air collector is more efficient. The finned collector with a 45° tilt angle had the maximum collector efficiency and air temperature rise. Show average temperature along the length of solar collectors versus panel thickness between 0 and 0.1 m for a single pass solar air heater in Figures 69, 70 and thickness of a solar collector versus the full area of the solar collector plates for a single pass solar air heater in Figures 69, 70 [62].

With the goal of enhancing heat transmission at the lee-side of the ribs, the heat transfer and flow parameters of six ribbed channels of square cross section with varied rib topologies are computed. Each channel's bottom walls are lined with six ribs. The pitch-to-height ratio (P/e) of ribs is 10. The downstream recirculating flow zone's shape has changed and its size has been compressed as a result of the diverse back-wall designs of ribs, while a small vortex near the downstream bottom corner of the rib and bottom wall has been destroyed. Heat transmission on the rib's back-wall area has greatly increased,

and this improvement is much more visible when the back-wall is extruded stream-wise. It is shown the distributions of

the normalized stream wise velocity contour line and the pressure coefficient for all situations in Figures 71, 72 [63].

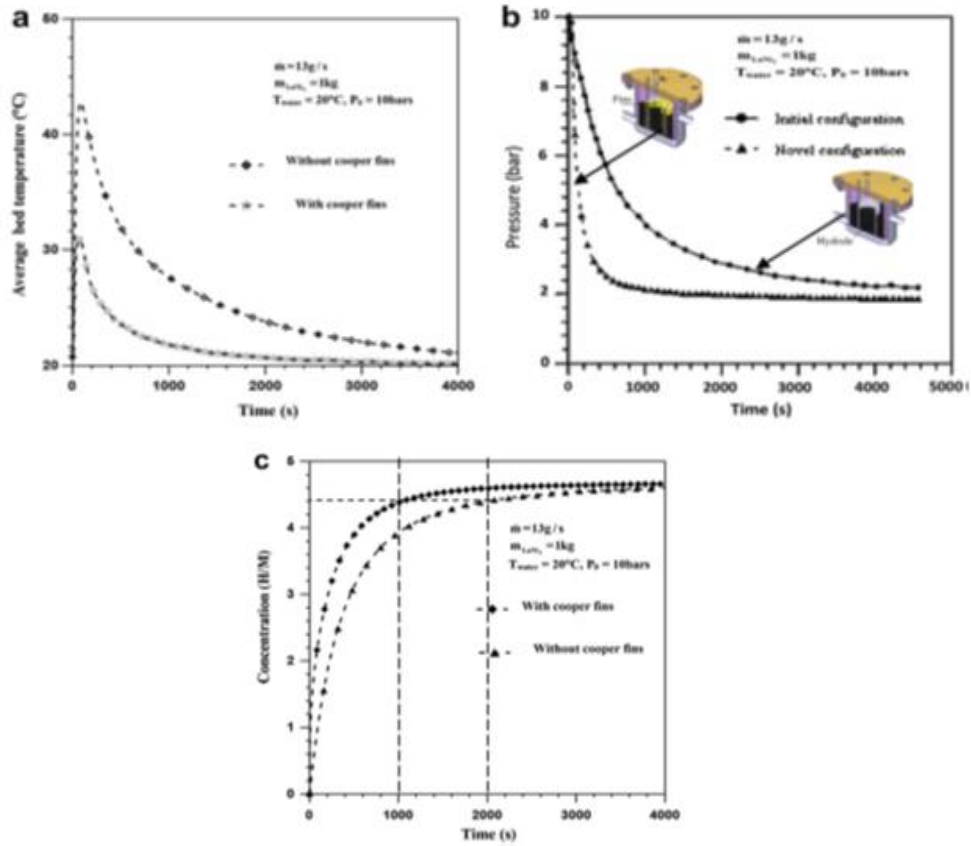


Figure 67. Effect of the copper fins on the absorption process [61]

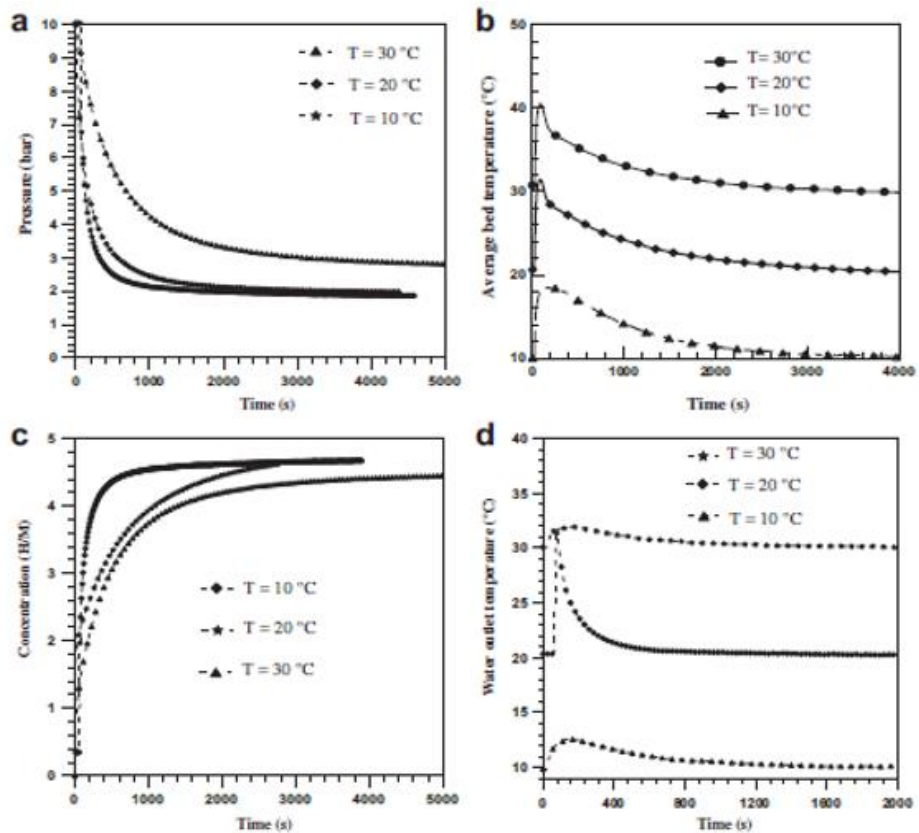
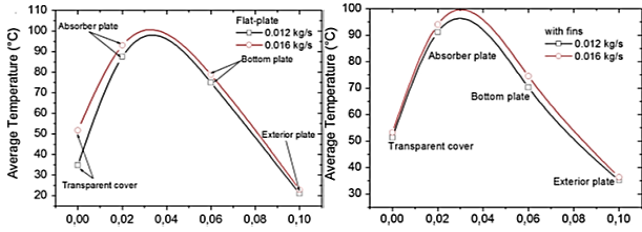
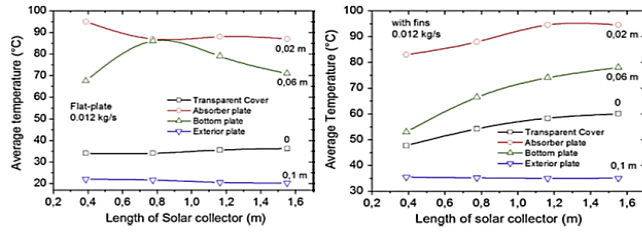


Figure 68. Effect of the water temperature on the absorption process [61]



**Figure 69.** Average temperature in the thickness of a solar collector versus the whole area of the solar collector plates for a single pass solar air heater, with flow rates of 0.012 and 0.016 kg s<sup>-1</sup>, for the solar collectors without using fins and with using fins [62]



**Figure 70.** Average temperature along the length of solar collectors versus thickness of panel of between 0 and 0.1 m for single pass solar air heater, at flow rates of (0.012, 0.016) kg s<sup>-1</sup>, corresponding to the flat-plate solar collector [62]

Discontinuous fin, staggered fin, and fin with vortex generator are three types of modified fin structures proposed to increase air side heat transfer of an air-cooled condenser in a power producing unit. The heat transmission capabilities of the extended wavy fins are investigated and compared to the original continuous wavy fins in a wind tunnel with a visible window for temperature distribution measurement of the fin surface. When the base tube wall temperature is constant, which is equivalent to the boundary condition of an air-cooled condenser, the area of current fin structures is redundant for heat loss capacity. As a result, all three upgraded fin types have higher overall heat transfer coefficients than the original continuous wavy fin, resulting in increased pressure drop. Show fin surface temperature distributions with air flow Reynolds number and heat transfer performance for four different types of fins in Figures 73, 74 [64].

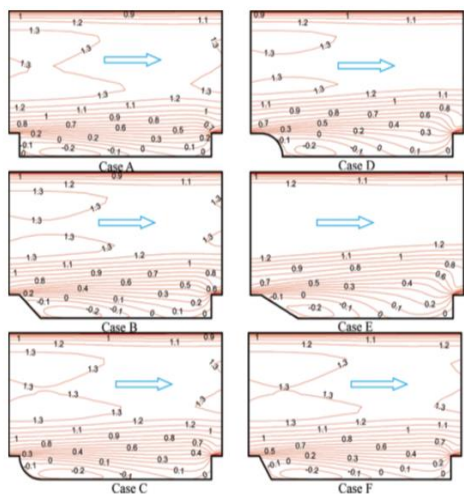


**Figure 71.** Distributions of normalized stream-wise velocity contour line between the 4<sup>th</sup> and 5<sup>th</sup> stream-wise rows of ribs for all cases, Re 1/4 16,000 [63]

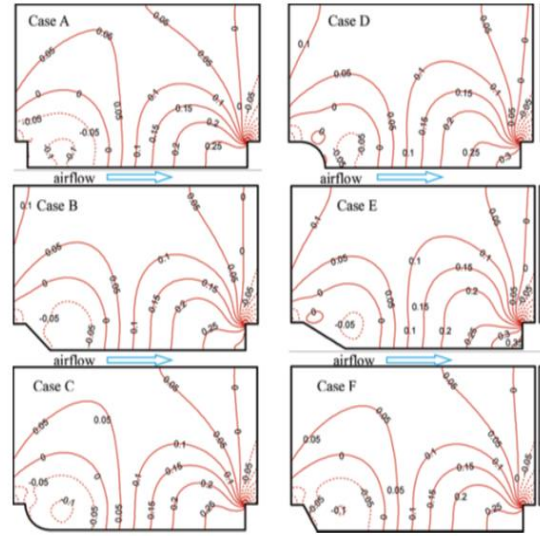


**Figure 72.** Distributions of the pressure coefficient between the 4<sup>th</sup> and 5<sup>th</sup> streamwise rows of ribs for all cases, Re 1/4 16,000 [63]

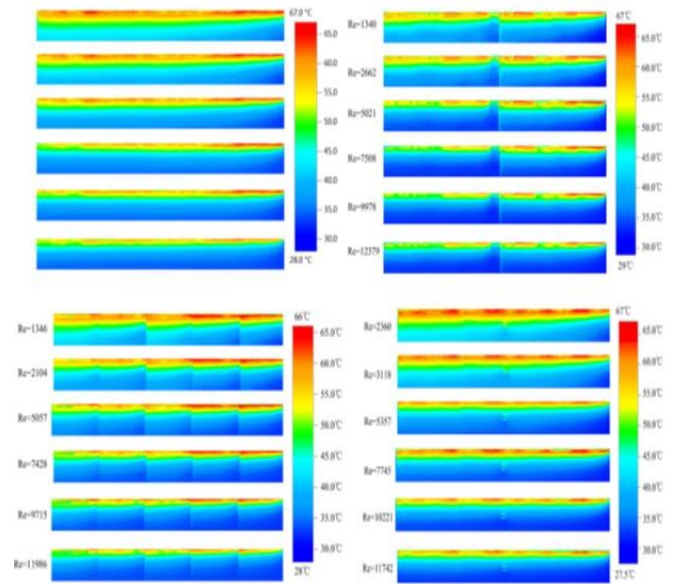


**Figure 73.** Fin surface temperature distributions with air flow Reynolds number. (a) Continuous wavy fin. (b) Discontinuous fin. (c) Staggered fin. (d) Fin with vortex-generator [64]

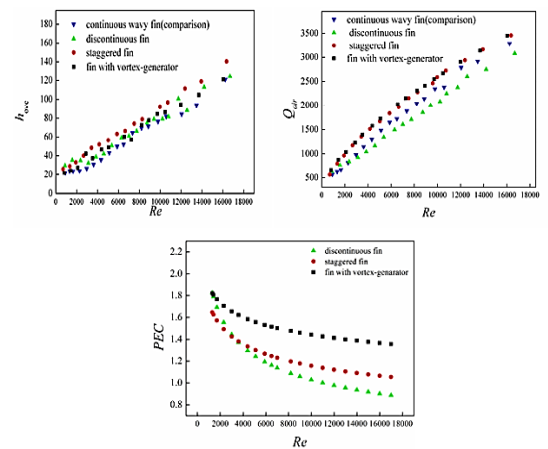


**Figure 74.** Heat transfer performances for four types of fins. (a) hove with Re. (b) P with Re. (c) Q<sub>air</sub> with Re [64]

With an operational temperature of 573 K and a nanoparticle concentration of 1% in volume, we offer a three-dimensional numerical analysis of heat transfer in a parabolic trough collector receiver with longitudinal fins utilizing several types of nanofluid. The following are the outcomes of this study: In contrast to smooth tube, the Nusselt number for absorber with fins insert ranged from 1.3 to 1.8 times. In comparison to plain tube, the friction factor for absorbers with fins ranged from 1.6 to 1.85. Heat transport is substantially improved by metallic nanoparticles compared to other kinds. When compared to smooth tube with base fluid, utilizing nanofluid in absorber with fins insert provides better heat transmission and thermo-hydraulic performance. Temperature distribution on the absorber inner wall's middle cross-section, Variation of local Nusselt number in a smooth tube, Effect of combining fins insert and nanofluid, and Thermo-hydraulic performance vs Reynolds number are shown in Figures 75-78 [65].

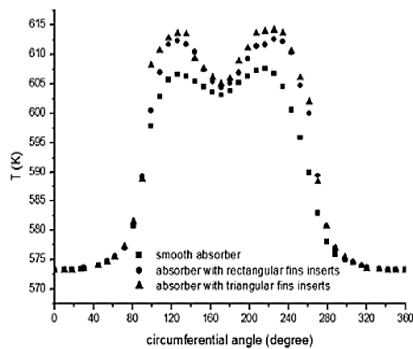


Figure 75. Temperature distribution on the middle cross-section of the absorber inner wall [65]

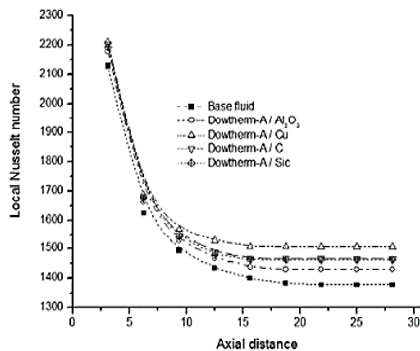


Figure 76. Variation of local Nusselt number in a smooth tube for  $Re=257056$  and  $\phi=0.01$  [65]

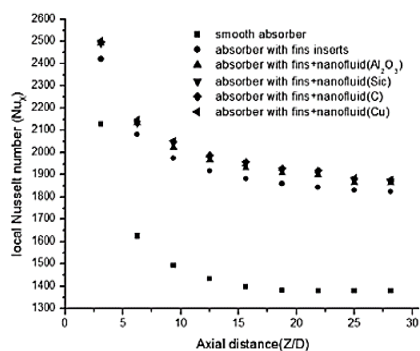


Figure 77. Effect of combining fins insert and nanofluid  $Re=257056$  and  $\phi=0.01$  [65]

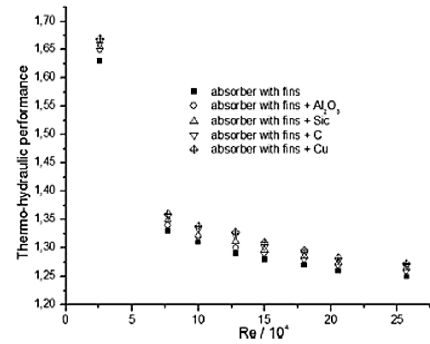


Figure 78. Thermo-hydraulic performance versus Reynolds number for  $T_{in}=573$  K and  $\phi=0.01$  [65]

Constructed theory presents a novel way for optimizing a wide range of engineering applications, including expanded surfaces and fins. The goal of this research is to develop and evaluate a cylinder with enhanced heat transfer surface area due to fins, utilizing Bejan's built theory notion. This study's findings may be deduced as follows: Total fin length for the three investigated fins should be in the range of 0.03 m to 0.1 m in order to transmit a higher rate of heat from the cylinder. For a given fin length, the heat transmission rate increased as the number of fin branches increased. In the diagram, show ideal Pareto fronts for various numbers of fin branches, design parameter distribution vs. rate of heat transfer for the optimal locations, and optimum Pareto fronts for both aluminum and copper as fin materials (Figures 79, 80) [66].

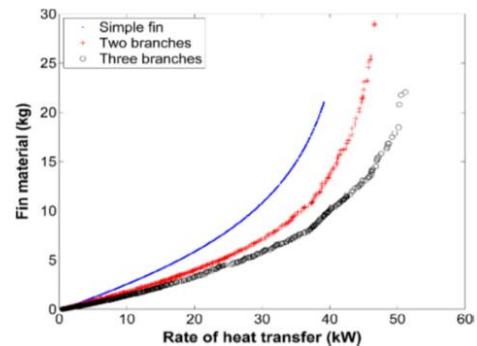


Figure 79. Optimum Pareto fronts for different number of fin branches [66]

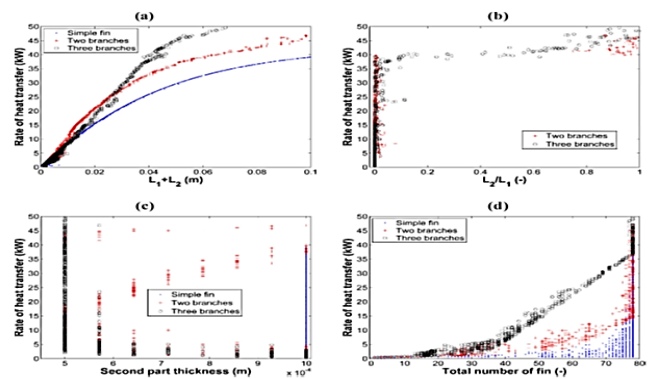


Figure 80. Distribution of design parameters versus rate of heat transfer for the optimum points in (a) Total fin length, (b) Ratio between the second and first part of fin length, (c) Fin second part thickness, and (d) Total number of fin [66]

The heat transmission of a cascaded thermal energy storage system with fins was investigated using an experimental setup. Rectangular, annular, and pin fins are welded within copper, brass, and stainless-steel encapsulating materials to improve heat transfer area. The finned encapsulations comprise three separate phase change materials: d-mannitol, d-sorbitol, and paraffin wax. Because circular finned encapsulated balls have a larger surface area than rectangular or pin fins, the PCM with annular finned encapsulated balls had a higher heat transfer rate from the HTF than other finned balls. It was also discovered that copper with annular finned balls had the best energy transmission, followed by stainless steel with annular fins. The findings of the investigation and the effect of utilizing fins on heat transport are shown in Figures 81, 82, 83, [67].

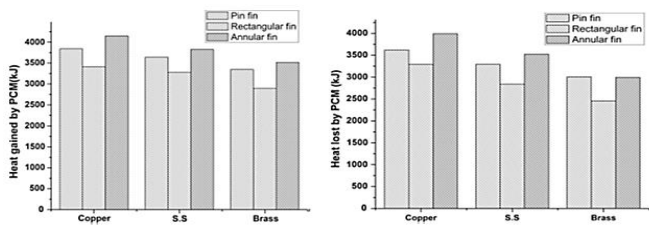


Figure 81. Heat gained and heat lost by d-mannitol [67]

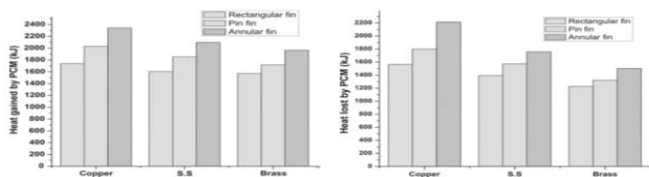


Figure 82. Heat gained and heat lost by d-sorbitol [67]

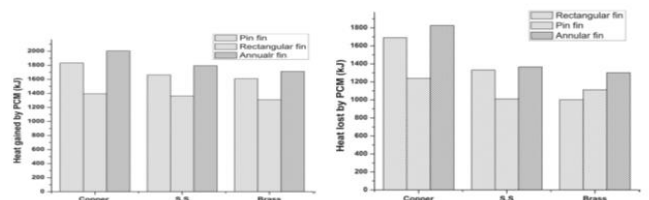


Figure 83. Heat gained and heat lost by paraffin wax [67]

A solar air heater is a device that converts solar energy into warmth. The heat absorption side of the solar air heater is changed with roughness ribs to boost its performance. The flow characteristics and heat enhancement caused by square shaped ribs in a solar air heater with a triangle cross-sectional channel were modelled using computational fluid dynamics (CFD). The  $Nu$  and  $f$  values are strongly influenced by the flow parameter. At higher  $Re$  levels,  $Nu$  has the highest value. Using square-shaped ribs resulted in a considerable increase in  $Nu$  and  $f$ . The maximum increase of 97% in  $Nu$  and 204% in  $f$  is found with the help of roughness [68]. The influence of a homogeneous external magnetic field on heat transfer enhancement of a fin-and-tube compact heat exchanger with  $Fe_3O_4$ /water Nanofluid is numerically explored. In the presence of a magnetic field, a magnetic force emerged around the tubes, forming vortices behind each tube, which increased the flow's mixing properties. As the magnetic field intensity rose, the local and average heat transfer coefficients increased around all tubes (particularly around the first and second tubes). In Figure 84, the average convective heat transfer coefficient, pressure drop, heat exchanger efficacy, and heat

exchanger efficiency are plotted against the Reynolds number at various magnetic field strengths [69].

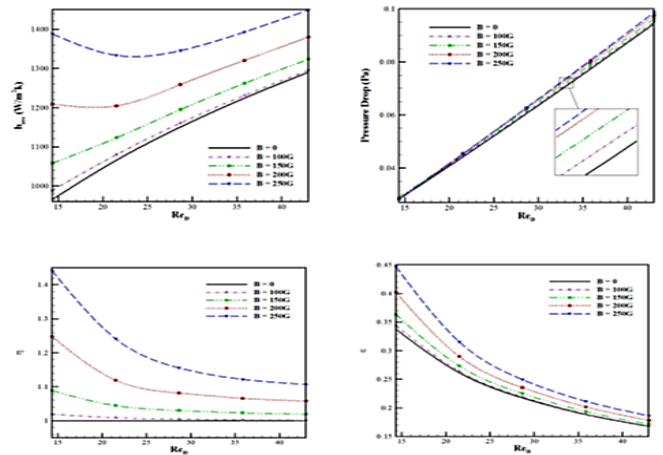


Figure 84. Variation of the average convection heat transfer coefficient, Pressure drop variation, heat exchanger effectiveness, and heat exchanger efficiency versus of the Reynolds number at different magnetic field intensities [69]

When compared to rectangular fins, rippling fins provide superior cooling performance. The base temperature of heatsinks with rippled fins is lower than heatsinks without rippled fins. The fins with one ripple (instance B) found to be the superior heat sink when compared to rectangular fins, delivering the best cooling performance and a mass reduction of 44%. When compared to Case A with rectangular fins, Case C has the highest mass reduction of 47.83%. When  $Q = 144W$  is employed, the mass specific heat transfer coefficient of the heat sinks  $h_m$  in examples B-F may be increased by 112.5%. Instances D and E were less efficient at higher heat fluxes. Figures 85, 86, 87, and 88 show schematic representations of various fin designs, temperature contours on the plane for various configurations, thermal resistance vs. heating power, and array heat transfer coefficient vs. heating power for various configurations [70].

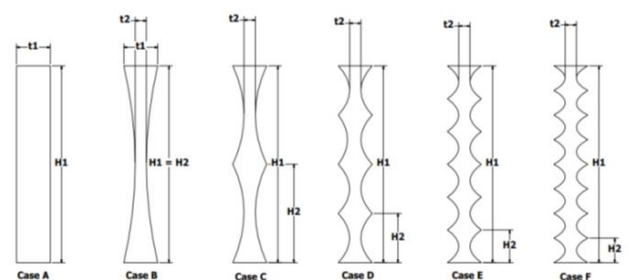


Figure 85. Schematic representation of different fin configurations considered in this study [70]

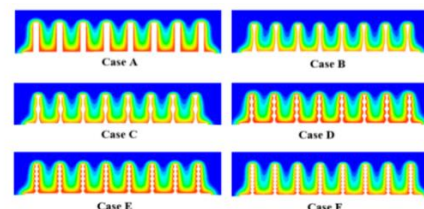


Figure 86. Temperature contour on the plane  $Y=0.15$  m for different configurations [70]

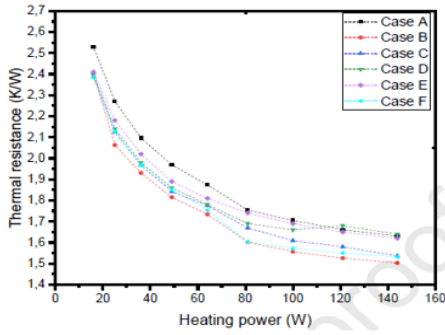


Figure 87. Thermal resistance versus heating power [70]

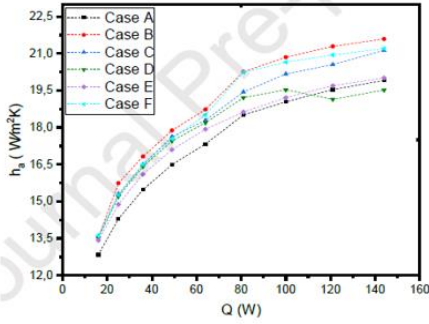


Figure 88. Array heat transfer coefficient versus heating power [70]

A new array of longitudinal fins was inserted at the interior circumference of a circular channel, which were not assembled consistently. Smooth, consistently finned, and non-uniformly finned channels were compared to one another while sharing the same pumping power. It has been demonstrated that the suggested non-uniform fin arrangement enhances thermal performance by up to 46% when compared to smooth and typical evenly finned channels [71].

Some innovative enhancements in wavy fin and tube heat exchangers' airside performance Waffle height, slits on wavy fins, and vortex generators are used to investigate the thermal resistance of wavy fin-and-tube heat exchangers. If the waffle height is increased, the thermal resistance will be reduced. The corrugation angle should be less than 15 and the waffle height should be less than or equal to the fin pitch. Wavy fins' heat transfer capacity can be improved by punching openings on top of leeward sections. When compared to punching slits on the top of leeward portions of wavy fins, punching slits on the top of leeward portions of wavy fins has no effect. For varied waffle heights and thermal resistance in various pumping power values, pressure drop and heat transfer characteristics for various widths and lengths of slits on top of wavy (Figures 89, 90) [71, 72].

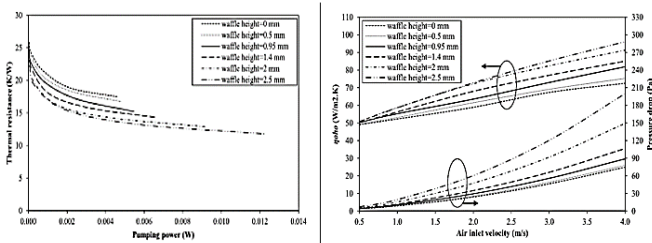


Figure 89. Comparisons of pressure drop and heat transfer characteristics for different waffle heights [71]

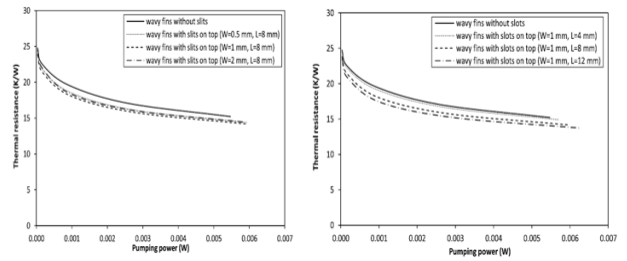


Figure 90. Thermal resistance in various pumping power values for different widths and lengths of slits on top of wavy fin-and-tube heat exchangers [72]

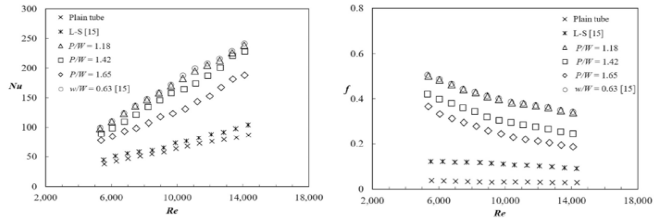
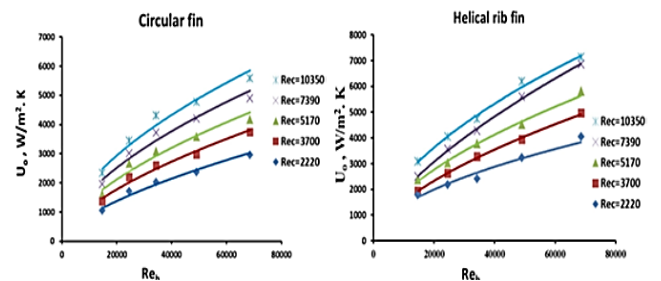


Figure 91. Correlation of Nu and f with Re representing the effect of P/W on Nu and f [73]

We've expanded our research to include a modified increased heat transfer area design for delta-wing tape inserts with a wing-pitch ratio (P/W) operating on the geometric characteristics. Characteristics of single-phase turbulent flow in a tubular heat exchanger with T-W inserts and P/W. Convective heat transport is considerably improved in tubes with T-W inserts. The present T-W insert with a P/W of 1.18 gives the largest heat transfer enhancement as compared to a plain tube and a tube with an L-S insert; Nu is enhanced by 177 and 145 percent, respectively.

The tube with T-W inserts and a P/W of 1.18 also has the highest f, which is 11.6 times greater than the plain tube and 2.72 times higher than the tube with an LS insert. Figure 91 depicts some of the study's findings [73].

In a double pipe heat exchanger, an experimental examination of heat transfers employing varied fin geometry for the heat exchange surface. Interrupted rectangular fins, circular fins, and helical ribs were among his fin geometries. When compared to a smooth tube, the rectangular fin gives the greatest heat transfer improvement, ranging from 68 to 168 percent depending on the flow conditions. When this form of fin is used, the pressure loss is significant. The heat transfer enhancement of the helical rib tube is lower (from 22 to 97 percent compared to the smooth tube) and the pressure drop is smaller than the rectangular fin. With just a 3–47 percent boost in heat transmission, the circular finned tubes give the predicted heat transfer advantage, but they also provide the lowest pressure drop. Figures 92 and 93 depict some of the study's findings [74].



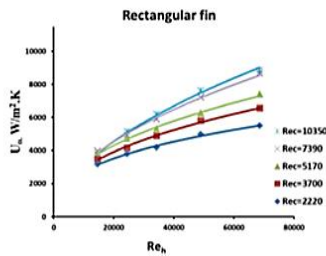


**Figure 92.**  $U_0$  versus  $Re_h$  at different  $Rec$  for two side circular, helical ribbed, and interrupted rectangular fin [74]

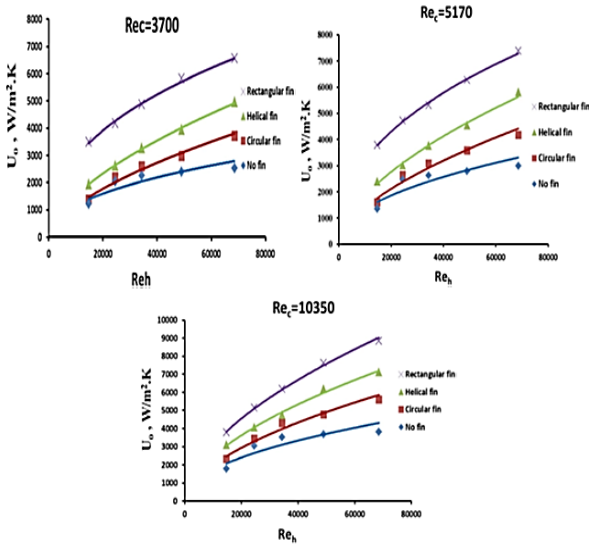


**Figure 93.**  $U_0$  versus  $Re_h$  at  $Re_c=(3700, 5170, 10,350)$  for different fins [74]

Porous fins multiply the surface area for convection, allowing more heat to move when compared to solid fins of the same size. This justifies its usage in applications where weight and material conservation are critical. Porous fins have a very nonlinear governing equation, making their analysis extremely difficult. The researchers are focused on determining the best fin profile as well as improving critical and sensitive factors. However, just a few examples of global optimization methodologies in the field of porous fins have been documented in the recent decade's archives [75].

At 293 K, a metal hydrides reactor was built and its heat transfer properties were quantitatively (finite volume technique) studied during hydrogenation and dehydrogenation of  $La_{0.9}Ce_{0.1}Ni_5$ . New internal copper fins and exterior water jackets are also included to boost heat transfer rates. For appropriate heat and mass transmission during hydrogenation and dehydrogenation processes in thermodynamic systems, a unique metal hydrides reactor with internal copper fins and an outside water jacket is designed and proposed. Internal copper fins result in rapid reaction kinetics as well as rapid heat removal from the process. It's also been discovered that as the number of fins, fin thickness, and fin height rise, so does the reaction kinetics and heat transmission. With the use of copper fins during absorption and desorption, he reduces the temperature of the average metal hydrides bed by 22.3 K and decreases the temperature by 6.8 K. Figures 94 and 95 demonstrate the fluctuation of hydrogen concentration with time during absorption as well as temperature contours with and without copper fins [76].

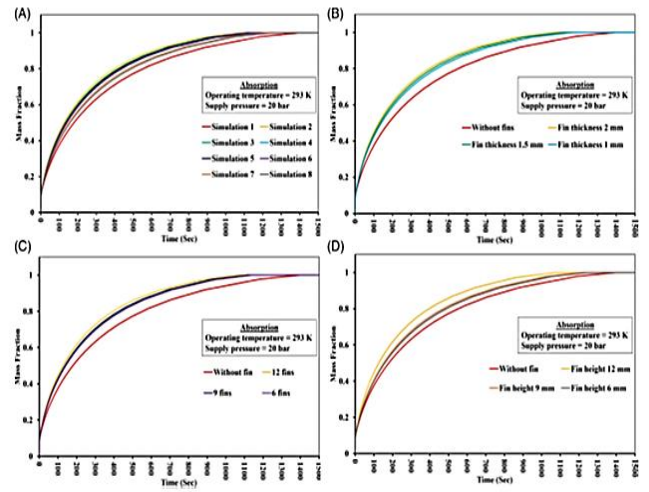


**Figure 94.** Variation of hydrogen concentration with time during absorption; (A) all variations, (B) at different fin thickness, (C) at different fin numbers and (D) at different fin height [76]

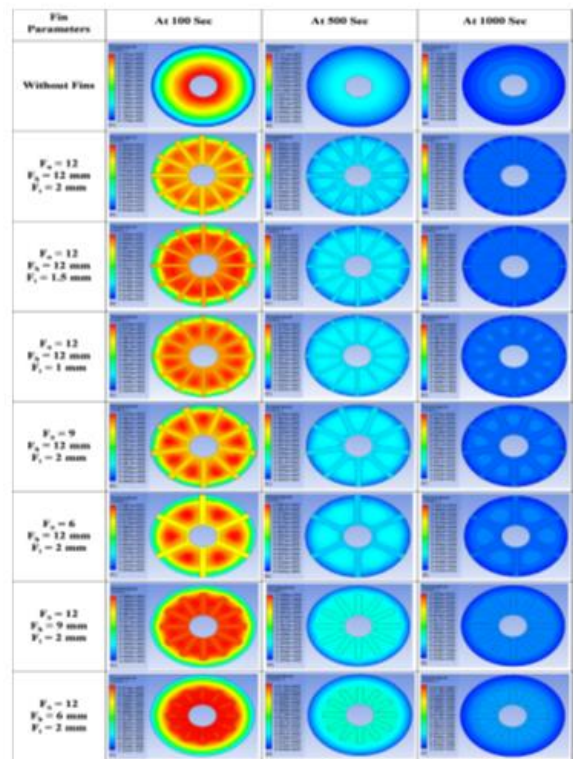


**Figure 95.** Temperature contours during absorption with and without copper fins [76]

Heat transfer can be enhanced by increasing the surface area of the heat exchanger and changing the direction of fluid flow. In micro-fin helically coiled tubes, heat transport and pressure decrease. It was observed that improving the performance of micro-fin helical tubes by reducing the Reynolds number and increasing the fin number was possible. The Nusselt number and pressure drop of the micro-fin helical coiled tube are higher than those of the smooth helical coiled tube. With the same Reynolds number ( $Re=20000$ ), the Nusselt number drops as the coil diameter of a micro-fin helical coiled tube grows [77]. A conjugate heat transfer model and complementing experimental are used to evaluate the benefits of numerous

holes and slots in a plate-fin heat sink. The heat transmission and pressure drop of the two new plate-fin heat sinks are investigated (with perforations and slots). The convection coefficient is improved by combining holes and slots. Plate fins with longitudinal holes and slots lose less pressure than those without. Novel fins are lighter than conventional fins because to their perforations and slots, which have a lower mass [78]. The performance of a double pipe heat exchanger with helical fins has been investigated experimentally. Heat exchanger performance in plain inner pipe is examined and compared to helical fins placed heat exchanger over inner pipe in terms of average heat transfer rate, heat transfer coefficient, and efficacy. When helical fins are utilized in place of smooth plain inner pipe in a heat exchanger, the heat transfer rate is found to be enhanced for practically all mass flow rates, and the increase is found to be 38.46 percent at higher mass flow rates. When a helical finned exchanger is utilized over the inner tube, the heat exchanger efficacy is 35 percent higher than when a smooth inner tube is employed [79, 80].

## 6. CONCLUSIONS

Where we note the great interest by researchers in developing heat transfer and using the best possible methods to improve heat transfer. In this literary review, a large group of research has been carried out to find out the importance of heat transfer and the methods used by researchers to develop heat transfer. Porous materials, nanomaterials and fins were used in the development of heat transfer. Where we note the importance of adding these materials (porous materials, nanomaterials and fins) to the original materials contribute significantly and clearly to improving heat transfer and this has a significant impact on energy consumption or trying to dissipate it, as we note the clear difference when using the original materials without adding these materials as the heat transfer is less and it consumes more time. Researchers can focus on the importance of improving heat transfer for its importance in many applications that have a direct impact on human life.

## ACKNOWLEDGEMENTS

The Presidency of Karbala University - Department of Construction, Projects, and the College of Engineering, supported this work.

## REFERENCES

- [1] Das, S.K., Choi, S.U., Patel, H.E. (2006). Heat transfer in nanofluids—A review. *Heat Transfer Engineering*, 27(10): 3-19. <https://doi.org/10.1080/01457630600904593>
- [2] Xuan, Y., Li, Q. (2000). Heat transfer enhancement of nanofluids. *International Journal of Heat and Fluid Flow*, 21(1): 58-64. [https://doi.org/10.1016/S0142-727X\(99\)00067-3](https://doi.org/10.1016/S0142-727X(99)00067-3)
- [3] Dhaidan, N.S., Khalaf, A.F. (2020). Experimental evaluation of the melting behaviours of paraffin within a hemicylindrical storage cell. *International Communications in Heat and Mass Transfer*, 111: 104476. <https://doi.org/10.1016/j.icheatmasstransfer.2020.104476>
- [4] Hussein, H.Q., Khalaf, A.F., Jasim, A.K., Rashid, F.L. (2021). Experimental investigation for the influence of a basement inside collector on solar chimney effectiveness. *Journal of Mechanical Engineering Research and Developments*, 44(4): 346-354.
- [5] Dhaidan, N.S., Khalaf, A.F., Khodadadi, J.M. (2021). Numerical and experimental investigation of melting of paraffin in a hemicylindrical capsule. *Journal of Thermal Science and Engineering Applications*, 13(5): 1-8. <https://doi.org/10.1115/1.4049873>
- [6] Kaggwa, A., Carson, J.K. (2019). Developments and future insights of using nanofluids for heat transfer enhancements in thermal systems: A review of recent literature. *International Nano Letters*, 9(4): 277-288. <https://doi.org/10.1007/s40089-019-00281-x>
- [7] Borode, A.O., Ahmed, N.A., Olubambi, P.A. (2019). A review of heat transfer application of carbon-based nanofluid in heat exchangers. *Nano-Structures & Nano-Objects*, 20: 100394. <https://doi.org/10.1016/j.nanoso.2019.100394>
- [8] Nikkam, N. (2014). *Engineering Nanofluids for Heat Transfer Applications*.
- [9] Liu, S., Sakr, M. (2013). A comprehensive review on passive heat transfer enhancements in pipe exchangers. *Renewable and Sustainable Energy Reviews*, 19: 64-81. <https://doi.org/10.1016/j.rser.2012.11.021>
- [10] Sivashanmugam, P. (2012). Application of nanofluids in heat transfer. *An Overview of Heat Transfer Phenomena*, 16. <https://doi.org/10.5772/52496>
- [11] Zhu, D., Yu, W., Du, H., Chen, L., Li, Y., Xie, H. (2016). Thermal conductivity of composite materials containing copper nanowires. *Journal of Nanomaterials*, 2016: 3089716. <https://doi.org/10.1155/2016/3089716>
- [12] Zhang, Y., Faghri, A. (2002). Heat transfer in a pulsating heat pipe with open end. *International Journal of Heat and Mass Transfer*, 45(4): 755-764. [https://doi.org/10.1016/S0017-9310\(01\)00203-4](https://doi.org/10.1016/S0017-9310(01)00203-4)
- [13] Yan, Y.Y., Lin, T.F. (1998). Evaporation heat transfer and pressure drop of refrigerant R-134a in a small pipe. *International Journal of Heat and Mass Transfer*, 41(24): 4183-4194. [https://doi.org/10.1016/S0017-9310\(98\)00127-6](https://doi.org/10.1016/S0017-9310(98)00127-6)
- [14] Sheikholeslami, M., Jafaryar, M., Said, Z., Alsabery, A. I., Babazadeh, H., Shafee, A. (2021). Modification for helical turbulator to augment heat transfer behavior of nanomaterial via numerical approach. *Applied Thermal Engineering*, 182: 115935. <https://doi.org/10.1016/j.applthermaleng.2020.115935>
- [15] Jadhav, M.M.P., Jadhav, D.B., Nimgade, M.E. (2017). Heat Transfer Enhancement using Nanofluids in Automotive Cooling System. pp. 1035-1042.
- [16] Buongiorno, J., Hu, L.W. (2009). Nanofluid heat transfer enhancement for nuclear reactor applications. In *International Conference on Micro/Nanoscale Heat Transfer*, 43918: 517-522. <https://doi.org/10.1115/MNHMT2009-18062>
- [17] Humnic, G., Humnic, A. (2012). Application of nanofluids in heat exchangers: A review. *Renewable and Sustainable Energy Reviews*, 16(8): 5625-5638. <https://doi.org/10.1016/j.rser.2012.05.023>
- [18] Li, Y., Shakeriaski, F., Barzinjy, A.A., Dara, R.N., Shafee, A., Tlili, I. (2020). Nanomaterial thermal

- treatment along a permeable cylinder. *Journal of Thermal Analysis and Calorimetry*, 139(5): 3309-3315. <https://doi.org/10.1007/s10973-019-08706-7>
- [19] Lotfizadeh, S., Matsoukas, T. (2015). Effect of nanostructure on thermal conductivity of nanofluids. *Journal of Nanomaterials*, 2015(2): 8. <https://doi.org/10.1155/2015/697596>
- [20] Moradi, A., Toghraie, D., Isfahani, A.H.M., Hosseini, A. (2019). An experimental study on MWCNT–water nanofluids flow and heat transfer in a double-pipe heat exchanger using porous media. *Journal of Thermal Analysis and Calorimetry*, 137(5): 1797-1807. <https://doi.org/10.1007/s10973-019-08076-0>
- [21] Delavar, M.A., Azimi, M. (2013). I using porous material for heat transfer enhancement in heat exchangers. *Journal of Engineering Science & Technology Review*, 6(1): 14-16. <https://doi.org/10.25103/jestr.061.03>
- [22] Liu, Z., Yao, Y., Wu, H. (2013). Numerical modeling for solid–liquid phase change phenomena in porous media: Shell-and-tube type latent heat thermal energy storage. *Applied Energy*, 112: 1222-1232. <https://doi.org/10.1016/j.apenergy.2013.02.022>
- [23] Yan, B., Wieberdink, J., Shirazi, F., Li, P.Y., Simon, T.W., Van de Ven, J.D. (2015). Experimental study of heat transfer enhancement in a liquid piston compressor/expander using porous media inserts. *Applied Energy*, 154: 40-50. <https://doi.org/10.1016/j.apenergy.2015.04.106>
- [24] Sheikhejad, Y., Hosseini, R., Avval, M.S. (2017). Experimental study on heat transfer enhancement of laminar ferrofluid flow in horizontal tube partially filled porous media under fixed parallel magnet bars. *Journal of Magnetism and Magnetic Materials*, 424: 16-25. <https://doi.org/10.1016/j.jmmm.2016.09.098>
- [25] Rashidian, S., Tavakoli, M.R. (2017). Using porous media to enhancement of heat transfer in heat exchangers. *International Journal of Advanced Engineering, Management and Science*, 3(11): 239937. <https://doi.org/10.24001/ijaems.3.11.5>
- [26] Pour-Fard, P.K., Afshari, E., Ziaei-Rad, M., Taghian-Dehaghani, S. (2017). A numerical study on heat transfer enhancement and design of a heat exchanger with porous media in continuous hydrothermal flow synthesis system. *Chinese Journal of Chemical Engineering*, 25(10): 1352-1359. <https://doi.org/10.1016/j.cjche.2017.01.015>
- [27] Shafii, M.B., Keshavarz, M. (2018). Experimental study of internal forced convection of ferrofluid flow in non-magnetizable/magnetizable porous media. *Experimental Thermal and Fluid Science*, 96: 441-450. <https://doi.org/10.1016/j.expthermflusci.2018.03.036>
- [28] Baragh, S., Shokouhmand, H., Ajarostaghi, S.S.M., Nikian, M. (2018). An experimental investigation on forced convection heat transfer of single-phase flow in a channel with different arrangements of porous media. *International Journal of Thermal Sciences*, 134: 370-379. <https://doi.org/10.1016/j.ijthermalsci.2018.04.030>
- [29] Baragh, S., Shokouhmand, H., Ajarostaghi, S.S.M. (2019). Experiments on mist flow and heat transfer in a tube fitted with porous media. *International Journal of Thermal Sciences*, 137: 388-398. <https://doi.org/10.1016/j.ijthermalsci.2018.11.030>
- [30] Moradi, A., Toghraie, D., Isfahani, A.H.M., Hosseini, A. (2019). An experimental study on MWCNT–water nanofluids flow and heat transfer in a double-pipe heat exchanger using porous media. *Journal of Thermal Analysis and Calorimetry*, 137(5): 1797-1807. <https://doi.org/10.1007/s10973-019-08076-0>
- [31] Talebizadeh Sardari, P., Walker, G.S., Gillott, M., Grant, D., Giddings, D. (2020). Numerical modelling of phase change material melting process embedded in porous media: Effect of heat storage size. *Proceedings of the Institution of Mechanical Engineers, Part A: Journal of Power and Energy*, 234(3): 365-383. <https://doi.org/10.1177/0957650919862974>
- [32] Aminian, E., Moghadasi, H., Saffari, H. (2020). Magnetic field effects on forced convection flow of a hybrid nanofluid in a cylinder filled with porous media: A numerical study. *Journal of Thermal Analysis and Calorimetry*, 141(5): 2019-2031. <https://doi.org/10.1007/s10973-020-09257-y>
- [33] Bairi, A., Alilat, N., Martín-Garín, A., Roseiro, L., Millán-García, J.A. (2021). Improving building's thermal performance by means of porous media—an experimental free convection work. *Heat Transfer Engineering*, 42(12): 1059-1066. <https://doi.org/10.1080/01457632.2020.1766252>
- [34] Moghadasi, H., Aminian, E., Saffari, H., Mahjoorghani, M., Emamifar, A. (2020). Numerical analysis on laminar forced convection improvement of hybrid nanofluid within a U-bend pipe in porous media. *International Journal of Mechanical Sciences*, 179: 105659. <https://doi.org/10.1016/j.ijmecsci.2020.105659>
- [35] Nazari, S., Ellahi, R., Sarafraz, M.M., Safaei, M.R., Asgari, A., Akbari, O.A. (2020). Numerical study on mixed convection of a non-Newtonian nanofluid with porous media in a two lid-driven square cavity. *Journal of Thermal Analysis and Calorimetry*, 140(3): 1121-1145. <https://doi.org/10.1007/s10973-019-08841-1>
- [36] Feng, X.B., Liu, Q., He, Y.L. (2020). Numerical simulations of convection heat transfer in porous media using a cascaded lattice Boltzmann method. *International Journal of Heat and Mass Transfer*, 151: 119410. <https://doi.org/10.1016/j.ijheatmasstransfer.2020.119410>
- [37] Pedrazzi, S., Allesina, G., Puglia, M., Morselli, N., Ottani, F., Parenti, M., Tartarini, P. (2021). Experimental heat transfer evaluation in a porous media. In *Journal of Physics: Conference Series*, 1868(1): 012016. <https://doi.org/10.1088/1742-6596/1868/1/012016>
- [38] Simon, N., Bour, O., Lavenant, N., et al. (2021). Numerical and experimental validation of the applicability of active-DTS experiments to estimate thermal conductivity and groundwater flux in porous media. *Water Resources Research*, 57(1): e2020WR028078. <https://doi.org/10.1029/2020WR028078>
- [39] Liu, P., Wang, P., Jv, L., Guo, Z. (2021). A coupled discrete unified gas-kinetic scheme for convection heat transfer in porous media. *Communications in Computational Physics*, 29(1): 265-291. <https://doi.org/10.4208/CICP.OA-2019-0200>
- [40] Rad, M.A.V., Kasaeian, A., Mousavi, S., Rajaei, F., Kouravand, A. (2021). Empirical investigation of a photovoltaic-thermal system with phase change materials and aluminum shavings porous media. *Renewable Energy*, 167: 662-675. <https://doi.org/10.1016/j.renene.2020.11.135>
- [41] Bairi, A. (2021). Using nanofluid saturated porous media

- to enhance free convective heat transfer around a spherical electronic device. *Chinese Journal of Physics*, 70: 106-116. <https://doi.org/10.1016/j.cjph.2020.03.023>
- [42] Gunnasegaran, P., Shuaib, N.H., Jalal, M.A., Sandhita, E. (2012). Application of nanofluids in heat transfer enhancement of compact heat exchanger. In *AIP Conference Proceedings*, 1502(1): 408-425. <https://doi.org/10.1063/1.4769160>
- [43] Lotfizadeh, S., Matsoukas, T. (2015). Effect of nanostructure on thermal conductivity of nanofluids. *Journal of Nanomaterials*, 2015(2): 8. <https://doi.org/10.1155/2015/697596>
- [44] Basem, A., Moawed, M., Abbood, M.H., El-Maghlany, W.M. (2022). The design of a hybrid parabolic solar dish–steam power plant: An experimental study. *Energy Reports*, 8: 1949-1965. <https://doi.org/10.1016/j.egyr.2021.11.236>
- [45] Razvarz, S., Jafari, R. (2018). Experimental study of Al<sub>2</sub>O<sub>3</sub> nanofluids on the thermal efficiency of curved heat pipe at different tilt angle. *Journal of Nanomaterials*, 2018: 1591247. <https://doi.org/10.1155/2018/1591247>
- [46] Sheikholeslami, M., Darzi, M., Sadoughi, M.K. (2018). Heat transfer improvement and pressure drop during condensation of refrigerant-based nanofluid; an experimental procedure. *International Journal of Heat and Mass Transfer*, 122: 643-650. <https://doi.org/10.1016/j.ijheatmasstransfer.2018.02.015>
- [47] Weng, H.C., Yang, M.H. (2018). Heat transfer performance enhancement of gravity heat pipes by growing AAO nanotubes on inner wall surface. *Inventions*, 3(3): 42. <https://doi.org/10.3390/inventions3030042>
- [48] Chen, L., Jafaryar, M., Shafee, A., Dara, R.N., Tlili, I., Li, Z. (2020). Effect of complex turbulator on heat transfer of nanomaterial considering turbulent flow. *Microsystem Technologies*, 26(3): 739-749. <https://doi.org/10.1007/s00542-019-04617-7>
- [49] Farshad, S.A., Sheikholeslami, M. (2019). Simulation of exergy loss of nanomaterial through a solar heat exchanger with insertion of multi-channel twisted tape. *Journal of Thermal Analysis and Calorimetry*, 138(1): 795-804. <https://doi.org/10.1007/s10973-019-08156-1>
- [50] Sheikholeslami, M., Jafaryar, M., Hedayat, M., Shafee, A., Li, Z., Nguyen, T.K., Bakouri, M. (2019). Heat transfer and turbulent simulation of nanomaterial due to compound turbulator including irreversibility analysis. *International Journal of Heat and Mass Transfer*, 137: 1290-1300. <https://doi.org/10.1016/j.ijheatmasstransfer.2019.04.030>
- [51] Gkoutas, A.A., Benos, L.T., Nikas, K.S., Sarris, I.E. (2020). Heat transfer improvement by an Al<sub>2</sub>O<sub>3</sub>-water nanofluid coolant in printed-circuit heat exchangers of supercritical CO<sub>2</sub> Brayton cycle. *Thermal Science and Engineering Progress*, 20: 100694. <https://doi.org/10.1016/j.tsep.2020.100694>
- [52] Chu, Y.M., Abohamzeh, E., Bach, Q.V. (2020). Thermal two-phase analysis of nanomaterial in a pipe with turbulent flow. *Applied Nanoscience*, pp. 1-12. <https://doi.org/10.1007/s13204-020-01576-8>
- [53] Sheikholeslami, M., Jafaryar, M., Sheremet, M.A., Shafee, A., Babazadeh, H. (2020). Nanomaterial thermal performance within a pipe in presence of turbulator. *Applied Nanoscience*, 10(9): 3421-3430. <https://doi.org/10.1007/s13204-020-01436-5>
- [54] Ahmed, W., Kazi, S.N., Chowdhury, Z.Z., et al. (2021). Experimental investigation of convective heat transfer growth on ZnO@ TiO<sub>2</sub>/DW binary composites/hybrid nanofluids in a circular heat exchanger. *Journal of Thermal Analysis and Calorimetry*, 143(2): 879-898. <https://doi.org/10.1007/s10973-020-09363-x>
- [55] Ajeel, R.K., Salim, W.I. (2021). Experimental assessment of heat transfer and pressure drop of nanofluid as a coolant in corrugated channels. *Journal of Thermal Analysis and Calorimetry*, 144(4): 1161-1173. <https://doi.org/10.1007/s10973-020-09656-1>
- [56] Chen, Y., Luo, P., He, D., Ma, R. (2021). Numerical simulation and analysis of natural convective flow and heat transfer of nanofluid under electric field. *International Communications in Heat and Mass Transfer*, 120: 105053. <https://doi.org/10.1016/j.icheatmasstransfer.2020.105053>
- [57] Kumar, S., Kumar, A. (2021). A comprehensive review on the heat transfer and nanofluid flow characteristics in different shaped channels. *International Journal of Ambient Energy*, 42(3): 345-361. <https://doi.org/10.1080/01430750.2018.1530139>
- [58] Kumar, S., Kumar, A. (2021). A comprehensive review on the heat transfer and nanofluid flow characteristics in different shaped channels. *International Journal of Ambient Energy*, 42(3): 345-361. <https://doi.org/10.1007/s10973-020-10261-5>
- [59] Singh, S.K., Sarkar, J. (2021). Improving hydrothermal performance of double-tube heat exchanger with modified twisted tape inserts using hybrid nanofluid. *Journal of Thermal Analysis and Calorimetry*, 143(6): 4287-4298. <https://doi.org/10.1007/s10973-020-09380-w>
- [60] Saeed, F.R., Al-Dulaimi, M.A. (2021). Numerical investigation for convective heat transfer of nanofluid laminar flow inside a circular pipe by applying various models. *Archives of Thermodynamics*, 71-95. <https://doi.org/10.24425/ather.2021.136948>
- [61] Dhaou, H., Khedher, N.B., Mellouli, S., Souahlia, A., Askri, F., Jemni, A., Nasrallah, S.B. (2011). Improvement of thermal performance of spiral heat exchanger on hydrogen storage by adding copper fins. *International Journal of Thermal Sciences*, 50(12): 2536-2542. <https://doi.org/10.1016/j.ijthermalsci.2011.05.016>
- [62] Chabane, F., Moumami, N., Benramache, S. (2014). Experimental study of heat transfer and thermal performance with longitudinal fins of solar air heater. *Journal of Advanced Research*, 5(2): 183-192. <https://doi.org/10.1016/j.jare.2013.03.001>
- [63] Zheng, S., Ji, T., Xie, G., Sundén, B. (2014). On the improvement of the poor heat transfer lee-side regions of square cross-section ribbed channels. *Numerical Heat Transfer, Part A: Applications*, 66(9): 963-989. <https://doi.org/10.1080/10407782.2014.894396>
- [64] Xu, C., Yang, L., Li, L., Du, X. (2015). Experimental study on heat transfer performance improvement of wavy finned flat tube. *Applied Thermal Engineering*, 85: 80-88. <https://doi.org/10.1016/j.applthermaleng.2015.02.024>
- [65] Amina, B., Miloud, A., Samir, L., Abdelylah, B., Solano, J.P. (2016). Heat transfer enhancement in a parabolic trough solar receiver using longitudinal fins and nanofluids. *Journal of Thermal Science*, 25(5): 410-417.

- <https://doi.org/10.1007/s11630-016-0878-3>
- [66] Hajabdollahi, Z., Hajabdollahi, H., Fu, P.F. (2017). Improving the rate of heat transfer and material in the extended surface using multi-objective constructal optimization. *International Journal of Heat and Mass Transfer*, 115: 589-596. <https://doi.org/10.1016/j.ijheatmasstransfer.2017.08.055>
- [67] Beemkumar, N., Karthikeyan, A., Yuvarajan, D., Lakshmi Sankar, S. (2017). Experimental investigation on improving the heat transfer of cascaded thermal storage system using different fins. *Arabian Journal for Science and Engineering*, 42(5): 2055-2065. <https://doi.org/10.1007/s13369-017-2455-9>
- [68] Kumar, R., Kumar, A., Goel, V. (2019). Performance improvement and development of correlation for friction factor and heat transfer using computational fluid dynamics for ribbed triangular duct solar air heater. *Renewable Energy*, 131: 788-799. <https://doi.org/10.1016/j.renene.2018.07.078>
- [69] Bezaatpour, M., Rostamzadeh, H. (2020). Heat transfer enhancement of a fin-and-tube compact heat exchanger by employing magnetite ferrofluid flow and an external magnetic field. *Applied Thermal Engineering*, 164: 114462. <https://doi.org/10.1016/j.applthermaleng.2019.114462>
- [70] El Ghandouri, I., El Maakoul, A., Saadeddine, S., Meziane, M. (2020). Design and numerical investigations of natural convection heat transfer of a new rippling fin shape. *Applied Thermal Engineering*, 178: 115670. <https://doi.org/10.1016/j.applthermaleng.2020.115670>
- [71] Hajmohammadi, M.R., Doustahadi, A., Ahmadian-Elmi, M. (2020). Heat transfer enhancement by a circumferentially non-uniform array of longitudinal fins assembled inside a circular channel. *International Journal of Heat Mass Transf.*, 158: 120020. <https://doi.org/10.1016/j.ijheatmasstransfer.2020.120020>
- [72] Sadeghianjahromi, A., Kheradmand, S., Nemati, H., Wang, C.C. (2020). Heat transfer enhancement of wavy fin-and-tube heat exchangers via innovative compound designs. *International Journal of Thermal Sciences*, 149: 106211. <https://doi.org/10.1016/j.ijthermalsci.2019.106211>
- [73] Wijayanta, A.T., Yaningsih, I., Juwana, W.E., Aziz, M., Miyazaki, T. (2020). Effect of wing-pitch ratio of double-sided delta-wing tape insert on the improvement of convective heat transfer. *International Journal of Thermal Sciences*, 151: 106261. <https://doi.org/10.1016/j.ijthermalsci.2020.106261>
- [74] Mohsen, O.A., Muhammed, M.A., Hasan, B.O. (2021). Heat transfer enhancement in a double pipe heat exchanger using different fin geometries in turbulent flow. *Iranian Journal of Science and Technology, Transactions of Mechanical Engineering*, 45(2): 461-471. <https://doi.org/10.1007/s40997-020-00377-2>
- [75] Deshamukhya, T., Bhanja, D., Nath, S. (2021). Heat transfer enhancement through porous fins: A comprehensive review of recent developments and innovations. *Proceedings of the Institution of Mechanical Engineers, Part C: Journal of Mechanical Engineering Science*, 235(5): 946-960. <https://doi.org/10.1177/0954406220939600>
- [76] Gupta, S., Sharma, V.K. (2021). Design and analysis of metal hydride reactor embedded with internal copper fins and external water cooling. *International Journal of Energy Research*, 45(2): 1836-1856. <https://doi.org/10.1002/er.5859>
- [77] Kumar, E.P., Solanki, A.K., Kumar, M.M.J. (2021). Numerical investigation of heat transfer and pressure drop characteristics in the micro-fin helically coiled tubes. *Applied Thermal Engineering*, 182: 116093. <https://doi.org/10.1016/j.applthermaleng.2020.116093>
- [78] Tariq, A., Altaf, K., Ahmad, S.W., Hussain, G., Ratlamwala, T.A.H. (2021). Comparative numerical and experimental analysis of thermal and hydraulic performance of improved plate fin heat sinks. *Applied Thermal Engineering*, 182: 115949. <https://doi.org/10.1016/j.applthermaleng.2020.115949>
- [79] Sivalakshmi, S., Raja, M., Gowtham, G. (2021). Effect of helical fins on the performance of a double pipe heat exchanger. *Materials Today: Proceedings*, 43: 1128-1131. <https://doi.org/10.1016/j.matpr.2020.08.563>
- [80] Basem, A., Moawed, M., Abboud, M.H., El-Maghlany, W.M. (2022). The energy and exergy analysis of a combined parabolic solar dish–steam power plant. *Renewable Energy Focus*, 41: 55-68. <https://doi.org/10.1016/j.ref.2022.01.003>